Music Visualization Using Projections to 2D Maps

A Thesis Proposal
Presented to
the Faculty of the College of Computer Studies
De La Salle University Manila

In Partial Fulfillment
of the Requirements for the Degree of
Bachelor of Science in Computer Science

by

CRUZ, Edwardo
DIONISIO, Jefferson
FUKUOKA, Kenji
PORTALES, Naomi

Fritz Kevin FLORES
Adviser

August 6, 2018

Abstract

Symphonies are musical compositions for orchestras that consist of several large sections called movements. There are five major musical periods namely the Baroque Period, Classical Period, 19th Century, Romantic Period, and the 20th Century that played a big role during the height of symphonies. This research will compare pairs of symphonies to determine their similarity, and create a visualization method to represent the comparison. From a previous research work by Azcarraga & Flores (2016) that compared symphonies though self-organizing maps (SOM), this research work will compare symphonies through visualization in a 3D SOM. By having a visual representation, the research provides an interactive and straightforward way to identify which parts of the symphonies are most similar and by adding the concept of time series on the clustering of the 3D SOM, more accurate results can be made. Quantitative data will be gathered through frequency cluster analysis and other statistical techniques to measure the musical trajectories of each musical segment of the symphony to produce the overall 3D SOM. T-SNE will also be experimented upon to see if it also produces optimal visualization for symphonies like with SOM.

Keywords: Machine Learning, Music, Time Dimension, Self-Organizing Map, K-Means Clustering.

Contents

Chapter 1

Research Description

1.1 Overview of the Current State of Technology

Music has been a part of peoples culture for hundreds of years, classical music being one of the oldest genres of music. Classical music is rooted in the traditions of early western music and to this day, many people refer to classical music as serious music. Musicians, however, use classical music to refer to music composed during 1750 to 1825, otherwise known as the Classical Era (Bernstein, 1959). The central norms of classical music became established between 1550 and 1900, which is known as the common-practice period. The common-practice period contains the majority of what we now know as classical music. Under this period there are 3 musical eras: Baroque, Classical and Romantic. Music from the Baroque period are decorated and elaborate, with little to no expression. Works from the Classical era contain repetitive dynamics and clean transitions. In contrast to music from the Baroque period, music from the Romantic period are expressive and emotive, having the ability to paint a vivid picture in the minds of the listeners (Grout & Palisca, 1996); however, Dahlhaus (1981) points out that another musical era existed between the Classical and the Romantic period and he refers to this as the 19th century era. This era serves as the transition period for the classical and romantic period, thus having similarities in style with both eras. After the common-practice period comes the 20th century era, which explores modernism, impressionism, neoclassicism and experimental music.

It was in the common-practice era when symphonies began to be composed. Libin (2014) describes symphonies as lengthy forms of musical compositions which are almost always written for orchestras and are consisting of several large movements. They are composed of three to five movements, depending on the time

period and are constructed by many different composers (Libin, 2014). There are five major musical periods namely the Baroque Period, Classical Period, 19th Century, Romantic Period, and the 20th Century. Musical pieces from each era share certain characteristics and styles that are representative of the era. With a history of almost 300 years, symphonies today are viewed as the very pinnacle of classical music where Beethoven, Brahms, Mozart and other renowned composers were able to find a venue for transcending their creativities and overall influencing them heavily on their music. During the course of the 18th century, the tradition was to write four-movement symphonies (Hepokoski & Darcy, 2006).

Throughout time, different styles have developed, each having features unique to themselves. Tilden (2013) notes the historical influence of composers with each other and how similar the methods of composing classical music are with pop music. As a result, symphonies written in the early 20th century may be influenced by the great composers and compositions of the previous eras. Analyzing these musical relationships and comparing one to another is a research area that could be done through both manual and machine learning methods.

McFee, Barrington & Lanckriet (2012) compare the use of context-based manual semantic annotation versus their proposed optimized content-based similarity learning framework. With machine learning, the use of high-quality training data without active user participation and the analysis of more data is possible than with feedback or survey data from active user participation. Human error in the analysis process can also be minimized with machine learning since human-supervised training is minimal. Corra & Rodrigues (2016) shows the analysis of music features using machine learning techniques. According to the MIR community (Silla & Freitas, 2009), the two main representation of music feature content are either audio-recorded or symbolic-based. The former employs the explicit recording of audio files while the latter uses symbolic data files such as MIDI or KERN.

SOMphony, a research paper by Azcarraga & Flores (2016), aims to understand the relationship of symphonies between the same composer to denote style as well as to determine the similarities between symphonies of different periods of music to denote influences between time periods. Their research showed the relationships and influences between composers from 5 major musical periods, namely the Baroque Period, Classical Period, 19th Century music, Romantic Period and the 20th century. Their research focused on self-organizing maps (SOM) that are trained using 1-second music segments extracted from the 45 different symphonies. The trained SOM is then further processed by doing a k-means clustering of the node vectors, allowing quantitative comparison of music trajectories between symphonies.

They used frequency counting in their research work for evaluation of each individual symphonies. Each time a 1 second music segment has a BMU inside a cluster, the frequency count for that cluster is incremented. In this way, only the clusters that are frequently visited or symphony will have a high frequency count. The frequency counts are then normalized by dividing the counts of a certain symphony by its total number of music segments. Once these normalized frequency counts are summarized, the resulting percentages can then be used to perform pairwise comparisons between symphonies.

Their research showed that using SOM is indeed helpful in visualizing the musical features of a symphony, making it easier to create insights about the relationships within the different pieces and composers. Their research concluded that a larger dataset would be needed to confirm whether the approach is indeed valid.

SOMphony, however, did not take into consideration the notion of time. In time dimension, each instance represents a different time step and the attributes give values associated with that time (Witten & Frank, 2005). To be able to generate time sensitive musical analysis, this research will add in the time dimension variable to the SOM and a new visualization in 3D space would need to be created.

In a research work by Maaten & Hinton (2008), they introduce a new visualization technique for assigning data points in a two dimensional or three dimensional map called t-Distributed Stochastic Neighbor Embedding or t-SNE, which is a variant of Stochastic Neighbor Embedding or SNE. Since t-SNE produces almost very distinct visualizations based on the experiment in their research work, this technique for visualizing individual symphonies may be more optimal than SOM in terms of both accuracy and efficiency.

1.2 Research Objectives

1.2.1 General Objective

To visualize symphonies using time dimension

1.2.2 Specific Objectives

The research aims to:

1. Perform feature selection to decrease number of features for faster training time in machine learning;
2. Find time-dependent distance measures to compare trajectories;
3. Create a 3D visualization model for the music data;
4. Determine feasibility of t-SNE as another form of visualization for comparison of symphonies;

1.3 Scope and Limitations of the Research

To be able to generate a self-organizing map, the proponents will use jAudio to extract 436 audio features from musical segments generated from the symphony (See Appendix C). The 436 audio features would be trimmed down through feature selection. By selecting only the n most influential features, the time it would take to train the SOM would not be as time consuming compared to using all 436 features, however, this may be at the cost of some of its accuracy in plotting the symphonys musical trajectory. In extracting the features, the musical piece is divided into 1 second music segments in order to be uniform all throughout the piece and to avoid incomplete notes. A 0.5 second overlap is used to be able to consider transitions between each second.

Different metrics for comparison will be used to evaluate which symphonies are similar. Together with the visual maps produced by either SOM or t-SNE, the proponents will then evaluate which metric shows results that reinforce the results seen from looking at the visual map. By doing this, the metrics that show more accurate results can be determined.

To create a 3D model to represent the symphony, the proponents will assign each generated SOM to a point in time and will be used to create a graph representing each map in a series. As a result of using the time dimension, this research will be able to better differentiate symphonies that use similar themes but at different periods of time in the composition.

Similar to SOMphony, the proponents will focus on representation of symphonies using SOMs for the purpose of comparison to other symphonies. T-SNE

will also be used as a visualization technique for the musical features of each symphony. The proponents will then decide which among the two to be used for metric evaluations depending on the results.

1.4 Significance of the Research

As the study focuses on qualitative comparison and analysis of different symphonies, the results of the study will prove that music is indeed quantifiable as opposed to being solely qualitative in nature.

The results of this study will also prove that the simplification of hours-long symphonies into a single visual representation in 3D space is possible. It can prove that visualization can be achieved, allowing comparison of data along the time dimension. The results of the study may also help prove the benefits and possibilities of SOM when transitioning from 2D to 3D using time. The results may also verify if t-SNE is a good visualization technique for comparison of musical data.

Some possible future application of the results of this study would include the improvement of existing music information retrieval (MIR) techniques used by music databases. Similarly, this research can also be used to further improve the algorithms used by playlist managers for the retrieval of similar songs from music databases using the comparison of the trained SOMs.

1.5 Research Methodology

This section contains phases and activities that will be performed to accomplish the research. The phases listed here will be arranged sequentially unless otherwise stated.

1.5.1 Concept Formulation and Review of Related Literature

This phase will concern the consolidation of the thesis requirements such as the objective of the research, the research problem to be tackled, and the scopes and limitations of such research. Research related to music comparison, machine

learning algorithms in music and music visualization will be part of the Review of Related Literature.

1.5.2 Data Gathering

This phase will concern the gathering of the additional symphonies to be used for the research. The original music dataset for SOMphony is composed of 75 symphonies spread across 5 periods each having 3 composers. To expand the dataset, 2 symphonies will be added to each composer, summing up to a total of 5 symphonies per composer and 2 composers will also be added for each era summing up to a total of 125 symphonies. The proponents have decided to maintain 5 symphonies per composer so that the data set will an equal number of symphonies per composer. The process of selecting which symphonies to be added would be by random to have a better grasp of the general style of the composer. The audio files would be retrieved from online sources and physical means. The researchers would not take into consideration the file type and bitrate of the audio files since music data that is free for use is limited.

1.5.3 Data Preparation

To prepare the data, the symphony audio files are converted into wav files in preparation for splitting. WaveSplitter will be used in splitting the audio file into 1 second segments at intervals of 0.5 second. These segments would undergo feature extraction using jAudio. The result would be an xml file containing all the features determined for each segment. The researchers would then run a RegEx script to remove the unnecessary text and format it into comma-separated values (CSV) file in preparation for labeling. Since the proponents would conduct supervised learning, the data needs to be labelled. The labelling scheme is as follows: period, composer, symphony and audio number (P1C1S1-0001).

The resulting CSV file was further cleaned by removing features that have the feature value 0 for all samples. Features that have at least one NaN value among its data was also removed. These features were removed since they were deemed to not be representative of the data. This leaves 276 features, from the original 534, to be used for training. Once completed, the the entire dataset is then normalized and clustered through Self-Organizing Maps.

1.5.4 Feature Selection

In this phase, the proponents will trim down the 436 features that jAudio has extracted. With decision trees, the top n nodes will be selected as the top n features. Principal component analysis (PCA), on the other hand, can be used to further reduce the number of features by merging columns that have similar data, until the dataset is only represented by a smaller number of features while still retaining the essence of the original data.. Aside from decision trees, the proponents will explore other statistical techniques such as PCA or Pearson correlation for feature selection which may prove more efficient or optimal than decision trees. By doing feature selection, the data set would have a uniform number of features for all symphonies and it would also enhance the efficiency of training the SOM.

1.5.5 Machine Learning and Similarity Metrics

This phase will concern training the SOM and t-SNE using the data with feature-selected features to reduce the dimensionality. The resulting maps can already be used to see similarities between composers, symphonies, or even musical periods. Different similarity metrics will be experimented and the results will be compared to the visual maps to see which metrics produce consistent results and to also be able to validate the similarities between the symphonies.

1.5.6 Visualization

The proponents will assign each BMU to a point on the generated SOM and this will be used to create a graph representing each map in a time series. As a result of using time dimension, the proponents will be able to better differentiate symphonies that use similar themes but at different periods of time in the composition. T-SNE will also be used as a secondary visualization technique for visualizing the symphonies to see if this technique will also provide good visualization for symphonies like with SOM.

1.5.7 Documentation

This phase will be done all throughout the whole research timeframe. The previously mentioned stages and their corresponding findings would also be documented duly.

1.6 Calendar of Activities

Table 1.1 shows the time table for the activities involved with the research for 2017 and Table 1.2 shows the activities for 2018. The numbers represent the number of weeks worth of activity. The # symbol represents the number of weeks allotted for the month.

Calendar of Activities							
Activities for 2017	Jun	Jul	Aug	Sep	Oct	Nov	Dec
Concept Formulation and RRL	###	####	#				
Data Gathering			#	###	##		
Data Preparation				##	##	####	##
Feature Selecion							
Machine Learning and Similarity Metrics				##	##	##	#
Visualization							
Documentation	##	###	##	###	####	####	##

Table 1.1 Timetable of Activities for 2017

Calendar of Activities							
Activities for 2018	Jan	Feb	Mar	Apr	May	Jun	Jul
Concept Formulation and RRL							
Data Gathering							
Data Preparation							
Feature Selecion	###	####					
Machine Learning and Similarity Metrics			####	####	####		
Visualization					####	####	
Documentation	###	####	####	####	####	####	##

Table 1.2 Timetable of Activities for 2018

Chapter 2

Review of Related Literature

This chapter discusses existing research on musical data representations. It also discusses the application of machine learning in music and visualization techniques for musical compositions. A summary of each section in this chapter is presented prior to the discussion of each section.

2.1 Musical Data Representation

Musical Data Representation and Interpretation			
Authors &Year	Title	Research Problem	Approach
Correa & Rodrigues (2016)	A survey on symbolic data-based music genre classification	Expanding music database needs more accurate tools for music information retrieval	Symbolic-based music feature are used to train system for genre classification.
McEnnis, McKay, Fujinaga, & Depalle (2005)	JAudio: A Feature Extraction Library	Solving existing problems in feature extraction systems	They developed jAudio to make extracting features a lot more convenient for researchers.
Cambouropoulos & Widmer (2000)	Automated Motivic Analysis via Melodic Clustering	Finding similarity in music patterns.	Their method uses differences in pitch-intervals and rhythm as basis for splitting one musical motive (small bits of music) from another.

As music grows continuously over time, a constant need for an upgrade to satisfy the number and size of music databases causes the development of more accurate tools for music information retrieval (MIR). MIR is the research field responsible for the development of algorithms or other computational means for the retrieval of useful information from music and the classification of music based on their categories. According to Corra & Rodrigues (2016), the ever increasing research on machine learning, the ever expanding abundance of digital audio formats, the growing quality and availability of online symbolic music data, and availability of tools for extracting musical properties motivate this study on machine learning and MIR. One of the main problems in MIR involves the classification of music based on their genre which this research work tackles. The automatic genre classification of music plays a key role in online music databases where websites or device music engines manage and label music content for retrieval. The main goal of this research work is to be able to compare music samples and give them their

own groups or tags in the database so that they can be easily retrieved whenever needed.

Symbolic-based data are music features extracted from symbolic data formats such as MIDI and KERN. In the MIR community, two main representations of music content for MIR research are followed, either the audio-recorded or the symbolic content. Audio-recorded content produce low-level and middle-level features, whereas symbolic content produce high-level features. When analyzing music content, it is preferable to extract more features with the high-level feature of the symbolic content since it is closer to the human perception of music. Due to these reasons, symbolic-based content is used for the research. This research further provides overviews of important approaches regarding music genre classification with the use of symbolic-based music features. The research, as a result, reveals that pitch and rhythm are the best musical aspects to be explored in symbol-based music feature classification that lead to accurate results. Some limitations for further improvement on future works however are present such as the small amount of music dataset used in the research, the bias of using western culture music, and the lack of comparison means for the result of the research due to the lack of previous research works regarding symbolic-based music genre classification.

McEnnis, McKay, Fujinaga, & Depalle (2005) introduced a feature extraction software for audio files called jAudio. jAudio provides an easy to use GUI and a command line interface for selecting which features to select/deselect from the list of features in jAudio's current library of feature extraction algorithms which can be found in Appendix C. The software accepts any audio file as input and outputs ACE XML or ARFF format for the features extracted from the audio file. The proponents in this research encountered many problems with regards to existing feature extraction softwares at the time of their research such as there was great difficulty in extracting perceptual features such as meter or pitch from a signal. Another problem was that there was no existing repository of feature extraction algorithms and researchers would have to implement their own feature extraction algorithm whenever they need it and there will be a big chance that they implement the algorithm incorrectly. There was also no existing feature extraction software that produced a standard output format. Feature extraction code was also restricted and not made available to users, thereby denying researchers from developing more feature extraction algorithms.

JAudio tackles these problems by being a Java-based software, making it easy to acquire and making it compatible with any platform. It produces a standard output format and handles dependencies well by executing all dependencies of a feature extraction algorithm before executing it. For example, the magnitude spectrum of a signal is used by a lot of other features so jAudio would prioritize extracting this first before the others to avoid repeating any extraction process.

JAudio also supports metafeatures which are just features that are used by all other features. Examples of this would be derivatives and mean.

Cambouropoulos & Widmer (2000) stated that music could be categorized into small bits called "motives". These motives are extracted from a musical piece by determining which clusters of musical data can be grouped together while maintaining melodic and rhythmic coherence. This is achieved by representing a melodic segment as a series of notes while minding musical closeness.

Their paper outlines a method that uses differences in pitch-intervals and rhythm as basis for splitting one musical motive from another. For example, two segments can be considered similar if they share a certain number of component notes or intervals using approximate pattern matching. The segments can also be considered similar if they contain shared elements at different pitches. However, this would require a more advanced pattern matching and data structure.

2.2 Machine Learning

Machine Learning			
Authors & Year	Title	Research Problem	Approach
Raphael (2010)	Music Plus One and Machine Learning	Computer driven musical accompaniment	Hidden Markov Models and Gaussian Graphical Models
Dubnov, Assayag, Lartillot, & Bejerano	Using Machine-Learning Methods for Musical Style Modeling	Predicting and determining musical context based on relevant past sample is very difficult because the length of the musical context varies widely	Two approaches, incremental parsing (IP) and the prefix suffix trees (PST), are used in designing predictors that can handle data with very large length.

Comparing trends in musical scores and generating a seemingly new work based on the past works of a certain composer has been the focus of another study. In Dubnov, et. al. (2003)'s research, they stated that predicting and de-

termining musical context based on relevant past samples is very difficult because the length of the musical context varies widely. The proponents formulated then that by using statistical and information theoretic tools, one can capture important trends present in the musical scores for further analysis with machine learning to derive mathematical models for inferring and predicting a seemingly new work from this particular composer. Large contexts make it very difficult to estimate because the number of parameters, computational costs, and data requirements for reliable estimation increases exponentially. To address this problem, the usage of predictors that can handle data with very large length is necessary. Two algorithms are used to design such a predictor for generating new works from old music scores, namely the incremental parsing (IP) and the prefix suffix trees (PST).

The IP algorithm was first suggested by Ziv & Lempel (1978). Given a string as input, the algorithm first builds a dictionary of distinct patterns by traversing from left to right of a sequence once and adding to the dictionary every time a new phrase with a different last character from the longest match that already exists in the dictionary. In representing the dictionary with a tree, every node contains a string in the dictionary and each time the algorithm reaches a node, it means that the string input contains the string assigned to the node but is longer. In this case, a new child node will be added to the tree.

PST was developed by Ron, Singer & Tishby (1996). This algorithm is very similar to IP, but it only adds to its dictionary if and only if the pattern or motif appeared a significant number of times in the string input and will prove to be useful in predicting for the future. Due to this, the main advantage that IP has over PST is that IP is a lossless compression algorithm, since in PST, some patterns are not added to dictionary, especially if they are not significant. PST, however, is more efficient that IP as a parsing algorithm.

Aside from music comparison, machine learning is also applied in automatic music accompaniment. These accompaniment systems serve as musical partners for live musicians that are performing music that is centered on the soloist. Raphael (2010) developed an accompaniment system with three modules namely Listen, Predict, and Play. The first module interprets the audio input of the live soloist in real-time, identifying note onsets with variable detection latency using hidden Markov model-based score following. However, there will be some detection latency due to the fact that a note must be heard first before it could be identified. To resolve this issue, the Predict module, implements a Gaussian graphical model that times the accompaniment on the human musician, continually predicting the evolution as more information comes.

2.3 Music Visualization

Musical Visualization			
Authors & Year	Title	Research Problem	Approach
Azcarraga, A., Caronongan, A., Setiono, R., & Manalili, S. (2016)	Validating the Stable Clustering of Songs in a Structured 3D SOM	Will constructing the classic 2D SOM as a 3D map be feasible, with the learning algorithm still the same as the 2D map?	The 3D map is designed as a $3X3X3$ cube with $9X9X9$ nodes. The cube is divided into one core cube and 8 corner cubes. The Euclidean distance from core to each corner represents the quality of the different categories or genres.
Barrington, Chan, & Lanckriet (2010)	Modelling Music as a Dynamic Texture	Addressing the lack of time-dependency between feature vectors	Dynamic Texture to represent a sequence of audio features
Maaten & Hinton (2008)	Visualizing Data Using t-SNE	To construct a dimensionality reduction visualization technique that can outperform other existing visualization techniques	Modify SNE to produce a more optimal visualization technique by replacing some steps in the algorithm like the cost function of SNE and by replacing the Gaussian distribution with Student t-distribution

Musical Visualization			
Authors & Year	Title	Research Problem	Approach
Foote (1997)	Visualizing music and audio using self-similarity	Is it possible to display the acoustic similarity between any two instants of an audio file as a two-dimensional representation	Audio similarity is computed by parameterizing them into MFCC's and getting the autocorrelation of two MFCC feature vectors V_i and V_j that were derived from audio windows.

Modeling music is representing the audio file in a machine-readable form. (Barrington et al., 2010) raises the issue of the lack of time dependency between feature vectors and stresses the need to have the feature vectors ordered in time. When time is ignored, the feature vectors fail to represent the musical dynamics of an audio fragment. The research addresses these limitations and proposes a visualization model for short temporal fragments of music and calls it a dynamic texture.

In another research work regarding the visualization of symphonies using SOM and also the previous research work this research work desires to expand on, Azcarraga & Flores (2016) focused on whether the music of certain composers and centuries are influenced by prior works of other composers. Their approach relied upon SOMs and k-means clustering where each section on the map represented a specific type of sound. When fed the data from a symphony, a line would be drawn and move from section to section which would represent the different types of sound the SOM would encounter during playback. The result would look like a scribble of lines superimposing each other. By comparing whether this signature of the symphony was similar to one of another symphony, the researchers were able to detect the stylistic influence that one composer has with another.

Azcarraga, Caronongan, Setiono, & Manalili (2016) presents a variant of the classical 2D SOM, a 3D SOM, that is stable with the general clusters not moving around on every training phase. A structured 3D SOM is an extension of a 2D Self-Organizing Map to 3D with a predefined structure. The 3D SOM is represented as a 3x3x3 cube with 27 sub-cubes of the same size. Each sub-cube is further divided into 9x9x9 nodes. The structured 3D SOM is a collection of

one distinct core cube in the center and 26 exterior cubes surrounding it, hence summing to a total of 27 sub-cubes. Alongside 3D SOM's built in structure, the learning algorithm used in this 3D SOM includes a four-phase learning and labelling phase. The first phase of training involves the semi-supervised training of the core cube. The second phase involves yet another semi-supervised training, but for the eight corner cubes. The third phase involves training the core cube again, but the training will be unsupervised. The fourth and final phase will be the labelling phase. This phase involves the uploading of the music files into the cube and labelling them accordingly. The music dataset used in this research includes songs from 9 genres: blues, country, hip-hop, disco, jazz, metal, pop, reggae, and rock. Each genre has 100 songs, thus summing to a total of 900 songs.

SOM is usually represented as a 2D map with the input elements being similar to the input environment. This research verifies that designing the SOM as a 3D map is very feasible, with the learning algorithm still the same as with the 2D map. By extending the SOM from 2D map to 3D, the map is further distinguished into the sub-cubes: eight corner cubes and one core cube in the center. Each corner cube represents a music genre while the core cube represents the song itself. The 3D SOM will be able to identify the quality of the different categories or genres of music albums based on a measure of distortion values of music files with respect to their respective music genres. Distortion value is measured by the Euclidean distance between the core cube and a corner cube.

Maaten & Hinton presents a visualization technique using dimensional reduction of high dimensional data into a 2D or 3D map called t-SNE as was briefly discussed in the introduction. This technique aims to transform high dimensional data into low dimensional data representation for data plotting in the map using a series of computational steps or algorithm which will be discussed in more detail in Chapter 3.

In their research work, they compared t-SNE with other techniques for dimensionality reduction for visualization of data which includes Sammon mapping, Isomap, and LLE using the MNIST data set, the Olivetti faces data set, and the COIL-20 data set. The resulting visualizations by t-SNE for all three types of data set proved to be superior to the three other techniques as t-SNE was able to cleanly cluster the different data classes together for each data set as compared to the other three techniques.

The main advantage of using t-SNE to other techniques is that t-SNE models dissimilar data points by means of large pairwise distances and models similar data points by means of small pairwise distances. This would result in a visual image that have similar data points grouped together and are far apart from data points that are very dissimilar with them. T-SNE also uses either of two tricks

which they label as early compression and early exaggeration. Early compression is when the map points are forced to stay together at the start of the optimization and early exaggeration is when map points are forced to have large gaps between their respective clusters by multiplying all of the high dimensional probabilities with a certain constant value so that the modelled data points will have larger values. When the data points are closely packed together in early compression, the clusters will be able to move much easier. Similarly, when there are large gaps among the different data points, the clusters will also be able to much easier to find a good global optimization.

Foote (1997) presented a paper on Visualizing Music and Audio using Self-Similarity. In this paper, the acoustic similarity between any two instants of an audio file is calculated and displayed as a two-dimensional representation. Structure and repetition is a general feature of nearly all music, with parts resembling certain parts of the song that came before it. This paper presents a method of visualizing the structure of the music by its acoustic similarity or dissimilarity in specific instances of time through grayscale gradation patterns.

Before getting the similarity measures, the two instants are first parameterized into Mel-frequency cepstral coefficients (MFCCs) plus an energy term. The similarity measure $S(i, j)$ is computed by getting the autocorrelation of two MFCC feature vectors V_i and V_j that were derived from audio windows. A simple metric of vector similarity S is the scalar product of the vectors. A better similarity measure can be obtained by computing the vector correlation over a window w. This captures the time dependence ofthe vectors. To have high similarity measure, the vectors must not only be similar, but their sequence must be similar as well.

Given the similarity measures $S(i, j)$ computed for all window combinations, an image is constructed so that each pixel at location (i, j) is given a grayscale value proportional to the measure. The maximum similarity measure is given maximum brightness. Visually, regions of silence or long sustained notes appear as bright squared on the diagonal. Repeated figures such as choruses and phrases will appear as bright off-diagonal rectangles. If the music has a high degree of repetition, it will show up as diagonal stripes or checkerboards that are offset from the main diagonal. Longer audio files would result to larger images due to the rapid rate of feature vectors. To reduce the image size, the similarity is only calculated for certain time indexes and since S is already calculated at window size w, the paper only looks at time indexes that are an integer multiple of w.

Chapter 3

Theoretical Framework

This chapter contains theories and concepts that are related to the research.

3.1 Symphonies

3.1.1 Basic Structure of a Symphony

The Classical and Romantic symphony is mainly written in four movements, namely the fast tempo or sonata allegro form, the slow tempo, the medium/fast tempo or minuet, and the fast tempo again. The sonata form makes up the main form of Classical and Romantic symphonies. It is composed of two contrasting themes, the aggressive and the passive and is further divided into several sections, namely the introduction, exposition, development, recapitulation, and coda. The introduction section is purely optional and is slow and solemn in nature. The exposition section is where the themes of the symphony are exposed or presented for the first time and will consequently be repeated all throughout. The development section is where the themes are altered and manipulated. The recapitulation section is where the themes return to their original forms from before they were altered. The code section finally represents the end of the movement and this is where the original tone from the exposition section is repeated or recapped to form the ending for the movement (Heikkinen, 2017 & BBC, 2014).

3.1.2 Music Features

A feature is a characteristic used to distinguish one entity from another and in a sense defines its uniqueness. Music features, therefore, are what makes music similar to or different from one another. By comparing the values for each music feature and by examining if a feature is present at all or not, comparison of music by mathematical means is very possible (Huron, 2001).

Today, music information retrieval (MIR) has become an important area of research especially because of the ever expanding database for music through the years. The features extracted from music can be used in many areas of MIR research. It can be said that when two songs share closer values for each music feature, then they are more similar than with others (Corra & Rodrigues, 2016).

MFCC

MFCC, also known as Mel-Frequency Cepstral Coefficients, is the most commonly used feature in speech analysis and since speech analysis and music research are closely interrelated as pointed out by Loughran, Walker, O'Neill, & O'Farrell (2008), then MFCC will likely be the most commonly used feature in music feature extraction.

According to Lutter (2014), MFCC is based mainly from experiments on human misconceptions of words such as when a person misunderstands what another person says. This feature extraction method was first developed by Bridle and Brown in 1974 and was further developed by Mermelstein (1976). The MFCC feature extraction method involves mimicking some parts of the human speech production and speech perception. This feature extraction involves five steps, namely the fourier transform, the mel-frequency spectrum, the logarithm, cepstral coefficients, and the derivatives. The first step, fourier transform makes use of the formula $C_{r,k} = |\frac{1}{N}\sum_{j=0}^{N-1} f j exp[-i2\pi\frac{jk}{N}]|$, where $k = 0, 1, ..., (\frac{N}{2}) - 1$ and N is the number of samples within a speech or time frame.

The mel-frequency spectrum closely mimics the sensation of the human ear's auditory system and the process involves filtering the spectrum with different band-pass filters, devices that pass frequencies within a certain range and reject all others, and the power for each band-pass filter is computed accordingly (Agarwal, 2017). The computation makes use of the formula $C_{T,j} = \sum_{k=0}^{\frac{N}{2}-1} d_{j,k}\, C_{T,k}$, where $j = 0, 1, ..., N_d$ and d is the amplitude of the band-pass filters at index j and frequency k, to produce the corresponding filter bank for the spectrum.

The third step, logarithm involves mimicking the perception of loudness by the human ear and is represented by the formula $C_{T,j} = log(C_{T,j})$ where $j = 0, 1, ..., N_d$.

In cepstral coefficients, the main goal here is to remove the speaker or the music dependent characteristics. The computation of cepstral coefficients results in the inverse of the fourier transform of the estimated spectrum of the signal and is represented by the formula $C_{T,j} = \sum_{j=1}^{N_d} C_{T,j}\, cos[\frac{k(2j-1)\pi}{2} N_d]$ where $k = 0, 1, ..., N_{m,c} < N_d$ and $N_{m,c}$ is the chosen cepstral coefficient for further processing.

Lastly, the derivative represents the dynamic nature of speech or the music.

3.2 Preprocessing

3.2.1 Data Collection

In gathering data, a careful lookup for patent or copyright issues must strictly be observed. Symphonies are musical pieces that were generally composed a long time ago and as such copyright on the actual symphonies are nonexistent. The only copyright issues to be possibly encountered here would be the source of the recreated symphony. For example, when the symphony is uploaded by a certain person in Youtube then the standard youtube license or the creative commons would apply (Brown, 2017).

3.2.2 Preparation of Dataset

In Azcarraga & Flores (2016)'s research regarding visualization and comparison of symphonies through SOM, the preparation of dataset was done by first cutting the symphony into multiple 1 second music segments with an overlapping interval of 0.5 second to provide a smoother transition of the segments when represented later visually in addition to taking consideration of sections or notes that have been abruptly cut during the splitting process. In this way, after the feature is extracted and trained in the SOM, the multiple music segments will make up different musical trajectories which makes up the map visualization.

3.2.3 Feature Extraction

Feature extraction is the means of extracting relevant and effective data to train machine learning algorithms. Not all features, however, may be useful and others may be irrelevant individually but can be useful when combined with other features. The input data or raw data often need to be converted into a set of useful features through preprocessing transformations such as, standardization, normalization, signal enhancement, nonlinear expansion, et al. The resulting data may also be pruned of excess features in order to achieve improved algorithm speed and or predictive accuracy (Guyon & Elisseeff, 2006).

Feature extraction for music can be done using jAudio, a Java project/program developed by McEnnis, McKay, Fujinaga, & Depalle (2005). JAudio is a feature extraction system that provides a user friendly GUI and a command line interface to suit user needs for selecting their desired features to be extracted for the audio. The system accepts audio files as input and outputs XML or ARFF files. This output file contains the values for each feature of the audio file selected by the user.

3.2.4 Feature Selection

Gupta (2017) defines decision tree as a binary tree that branches down from the root. The term tree-walking is used to continuously make decisions on every level of the tree starting from the root node until the leaf nodes are reached or a satisfactory answer is found. In this way, it can be derived that the nodes found at the top of the tree are more important than its child nodes and all others beneath them. Decision trees are useful for inferring what features of a dataset can greatly or weakly influence its outcome (Mitchell, 1997).

Feature selection is the automatic selection of attributes in the dataset that are most relevant to a specific predictive model. It seeks to identify the out of the ordinary features among all the others and it helps in reducing the number of data attributes being used while still retaining a good or accurate predictive model. Aside from reducing the number of features or data attributes, it can also help in removing unwanted attributes that may decrease the accuracy of the predictive model (Brownlee, J., 2014).

Grabczewski & Jankowski (2005) explains that decision tree algorithms are best used for feature selection because of the inherent characteristic of decision trees that allows them to separate the different features and showcase the more important features since it will appear at the root of the decision tree.

Some simple but successfully tested algorithms for feature selection would include Pearson's correlation coefficient and Fisher-like criterion. Pearson's correlation coefficient or Pearson's R is widely used in the computation of statistics and this involves detecting linear correlation, which is the representation of how close the data points are in making a straight line in a graph, just as shown in Figure 3.1.

Figure 3.1: Pearson Correlation Graph

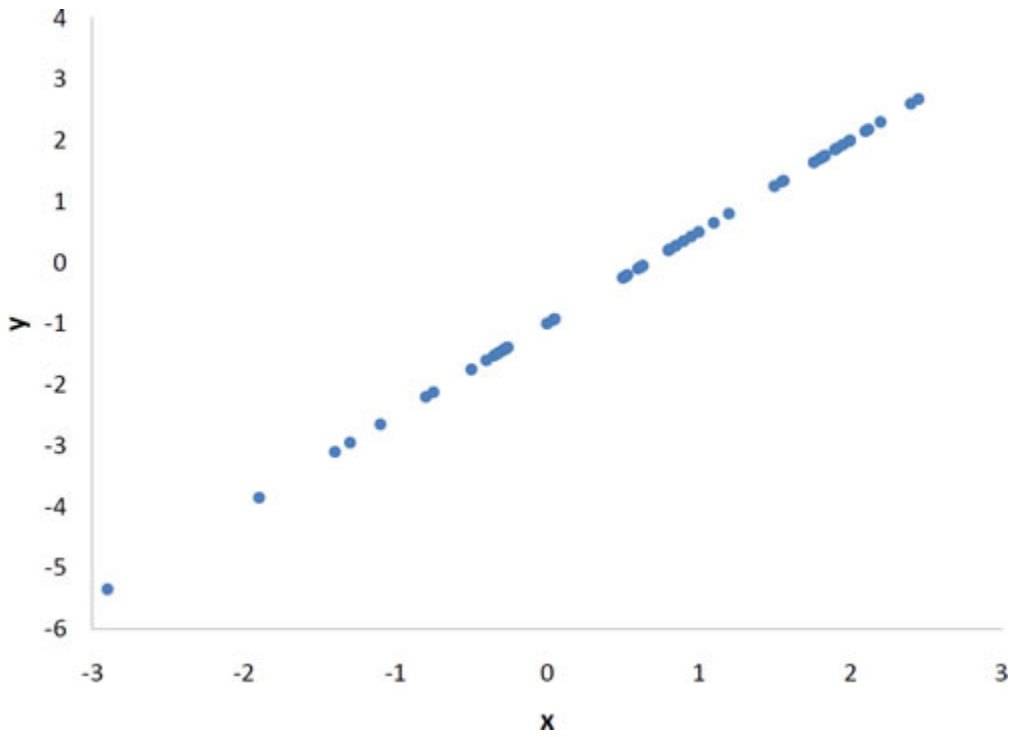

PCA is another statistical procedure that transforms a set of data points using orthogonal transformation, which scales the set of points by a certain value, into a set of linearly uncorrelated values called principal components. Principal components are ordered such that the variance from the original variable decreases. It will always turn out that the first principal component will have the largest variance that was present in the original variable.

In machine learning, PCA is used to reduce the dimensionality of a set of data points. In implementing PCA on a 2D data set, the mean and the covariance of the data set would first have to be computed first. Mean is computed using $m = \frac{1}{P}\sum_{\mu=1}^{p} x^{\mu}$ and Covariance is measured using $S = \frac{1}{P-1}\sum_{\mu=1}^{P}(x^{\mu} - m)(x^{\mu} - m)^{T}$ (Storkey, 2017).

The eigenvalue and the eigenvector would also have to be computed. Eigenvector is computed using the formula $det(\lambda I - A) = 0$, where λ is the eigenvalue,

I is the identity matrix of A, det is the determinant of the matrix, and A is the covariance matrix from the previous step. Eigenvalue is computed using the formula $(\lambda I - A)v = 0$.

For each data point x^n, the lower dimensional representation is $y^\mu = E^T(x^\mu - m)$ and the approximate reconstruction of the original data point x^n is $x^\mu = m + Ey^\mu$. The total squared error over all the training data made is given by $(P-1)\sum_{j=M+1}^{N} \lambda j$ where $\lambda j, j = M+1...N$ are the eigenvalues discarded in the projection.

The last step is to choose the components and to form the feature vector. The number of eigenvectors and eigenvalues is equal to the number of data in the dataset. The eigenvector corresponding to the highest eigenvalue is the principal component of the dataset. To form the feature vector, the top k eigenvectors with top eigenvalues will be used. To compute for the principal component, the transposed version of the feature vector is left-multiplied with the transposed version of the scaled version of the original dataset.

Fisher-like criterion makes use of the formula $\frac{m_0 - m_1}{s_0 - s_1}$, wherein m is the mean value of the feature for the$i$-th element and s is the corresponding standard deviation. This algorithm can only be used, however, when dealing with binary classifications.

Feature selection, in general however, can be classified into three categories, namely the filter methods, wrapper methods, and the embedded methods. Filter method involves labelling each feature with a statistical measure and by comparing these measures, the more important features can be selected. Wrapper method involves grouping different combinations of features together to see which combinations work best. Embedded methods involve learning which features best contribute to the accuracy of the model while the model is simultaneously being created. Some more examples of feature selection algorithms would include best-first search, hill-climbing algorithm, and the usage of heuristics. Best-first search and hill-climb fall under the wrapper methods wherein different combinations are used until the top n features are found. Heuristics falls under the filter method wherein a heuristic score is given to each feature using a statistical measure such as Euclidean distance for example, and the features with the high scores will be the ones selected.

3.3 Machine Learning

Machine learning as defined by Ng (2017) is the science behind computers acting on a certain stimulus without being explicitly programmed to do so. Some examples of impact led by machine learning would be self-driving cars and web search suggestions from Google. Machine learning is also widely used in many different fields of research such as in artificial intelligence, data mining, natural language processing, image recognition, and expert systems (McCria, 2014). In machine learning, the concept of training the system to perform a unique task given a certain amount of data received has two main underlying categories, unsupervised learning and supervised learning.

3.3.1 Supervised Learning

Supervised learning, as defined by Brownlee (2016), is a type of machine learning wherein an input variable and an output variable is defined and an algorithm is used to map the input to the output variable. The goal of this type of learning is to map the input variables to their respective output variables by approximation so that when a new input variable is presented, an output can be predicted by the system. The main difference of supervised learning over unsupervised is that there is no third party that supervises and corrects the training of data in unsupervised but in supervised, intervention of the supervisor is necessary in order to achieve an acceptable level of performance by the system. Supervised learning can be further divided into two groups, namely regression and classification. Regression is used when the output is a real value, for example, weight, height, or age. Classification is used when the output is a category or group, for example, colors, sizes.

3.3.2 Unsupervised Learning

Brownlee (2016) defines unsupervised learning as having no corresponding output variable. Unsupervised learning is analysing the structure and distribution of the data in order for system to learn. Unsupervised learning can be further classified into two groups of algorithms, namely the clustering and the association. Clustering is used for discovering the groupings of data through clusters and association is used for discovering rules that describe the provided data.

SOM

Teuvo Kohonen (1995) defines SOM as a data visualization technique developed by Professor which reduces the dimension of data through the use of self-organizing neural networks. As SOM reduces the dimension of data, it also groups similar data items together; therefore, it not only reduces the dimension of data but also groups similar ones together. Figure 3.2 shows a basic example of a SOM. Note in this example that the data represented by colors are grouped according to their similarity (eg. yellow is near orange, dark teal is between blue and green).

Figure 3.2: SOM Sample

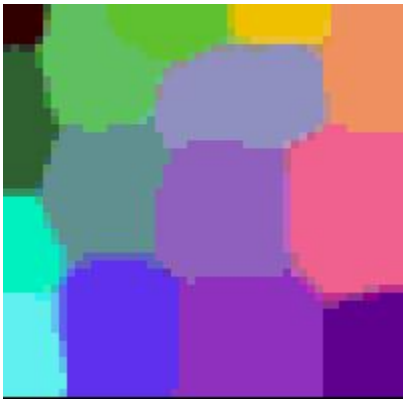

Rumelhart & Zipser (1985) defines a class under supervised learning called competitive learning. Here, neurons compete among themselves in a winner-takes-it-all scenario wherein only one neuron wins and is activated at any one time. Implementation of this competition is done through the use of lateral inhibition connections, which are structures of a network in which neurons inhibit their neighbors. When neurons are forced to organize themselves through this scenario, then the result would be a map that is self-organized, thus a SOM.

K-Means Clustering Algorithm

K-means clustering algorithm is a type of unsupervised learning algorithm wherein a set of unlabeled data will be grouped together and these groups are defined as the k variable. The algorithm will assign the different data points to their respective k-groups based on the selected features. Data points will then end up being clustered based on their feature similarities. The algorithm has two main iterative steps, , the data assignment step and the centroid update step, that repeats until either data points change clusters, the sum of the distances is minimized, or some maximum number of iterations is reached. Before starting

with these two steps, the centroid for each k-cluster is computed first. In data assignment, each data point is placed in their nearest centroid value computed with squared Euclidean distance. In centroid update, the centroid is recomputed by taking the mean of all the data assigned to the cluster of the centroid (Hartigan & Wong, 1979).

t-SNE

Maaten & Hiton (2008) introduces t-SNE as a variant of the Stochastic Neighbor Embedding (SNE), which seeks to visualize high dimensional data by plotting these data points in a two or three dimensional map. Since t-SNE is a variant of SNE, SNE would have to be discussed first before transitioning to t-SNE. SNE starts by transforming the Euclidean distances of the high-dimensional data points into conditional probabilities that represent similarities. For example with $p_{j|i}$, this would represent the similarity from X_j to X_i, that X_i would pick X_j as its neighbor if neighbors were picked in proportion to their probability density under a Gaussian centered at X_i. The conditional probability of $p_{j|i}$ is given with $p_{j|i} = \frac{exp(-||x_i - x_j||^2/2\delta_i^2}{\sum_{k \neq i} exp(-||x_i - x_k||^2/2\delta_i^2}$ where δi is the variance of the Gaussian that is centered in X_i. $p_{i|i}$ is set to 0 since only pairwise similarities will be considered. For the low dimensional counterpart of X_i and X_j, the probability is computed by $q_{j|i} = \frac{exp(-||y_i - y_j||^2}{\sum_{k \neq i} exp(-||y_i - y_k||^2)}$.

As with its high dimensional counterpart, $q_{i|i}$ is set to 0. In order for SNE to find a low dimensional data representation that represents the mismatch between $p_{j|i}$ and $q_{j|i}$, a cost function is used, $C = \sum_i KL(P_i||Q_i) = \sum_i \sum_j p_{j|i} log \frac{p_{j|i}}{q_{j|i}}$,where KL is the Kullback-Leibler divergences, P_i is the conditional probability distribution over all other data points given data point X_i, and Q_i is the conditional probability distribution over all other data points given data point Yi.

With the variance δi of the Gaussian that is centered over each high-dimensional data point X_i, it is important to note that the density of all data points in a data set are not uniform and it is more appropriate to use a smaller δi value in denser regions than in sparser regions. Any value of δi influences a probability distribution P_i over all other data points. This probability distribution has an entropy value which increases as δi increases. SNE seeks for a value of δi that has a P_i with fixed perplexity specified by the user using binary search. The perplexity is computed by $Perp(P_i) = 2^{H(P_i)}$ where the $H(Pi)$ or the Shannon entropy of P_i is further computed using $H(P_i) = -\sum_j p_{j|i} log_2 p_{j|i}$. The smooth measure of the effective number of neighbors can also be identified as the perplexity and the typical values for this would range from 5 to 50. The cost function shown earlier

can also be minimized into $\frac{\delta C}{\delta y_i} = 2\sum_j (p_{j|i} - q_{j|i} + p_{i|j} - q_{i|j})(y_i - y_j)$.

The gradient can be thought of as a spring force from a map point y_i to any y_j along the map. As the force is computed with $y_i - y_j$, the resulting force can either make the points repel or attract each other depending if the distance between the two is too small or too large. To speed up the optimization and to avoid poor local minima, a gradient update with a momentum term is done using $y^{(t)} = y^{(t-1)} + \eta\frac{\delta C}{\delta y} + \alpha(t)(y^{(t-1)} - y^{(t-2)})$ where y^t indicates the solution at iteration t, η indicates the learning rate, and $\alpha(t)$ represents the momentum at iteration t.

In t-SNE, certain issues such as the crowding problem, which is when too many data points get crowded in a map with a small number of dimension such as with 2D or 3D, are tackled by using a symmetrized version of the SNE cost function with more simple gradients and to use Student t-distribution instead of the Gaussian distribution when computing similarity between two low-dimensional points. The alternative cost function for a symmetrized SNE is $C = KL(P||Q) = \sum_i \sum_j p_{ij} log\frac{p_{ij}}{q_{ij}}$ where $p_{i|i}$ and $q_{i|i}$ are set to 0 just as in SNE and $p_{ij} = p_{ji}$ as $q_{ij} = q_{ji}$ since they constitute the symmetric property. p_{ij} is computed using $p_{ij} = \frac{exp(-||x_i - x_j||^2/2\delta^2)}{\sum_{k\neq 1} exp(-||x_k - x_l||^2/2\delta^2)}$ and q_{ij} using $q_{ij} = \frac{exp(-||y_i - y_j||^2)}{\sum_{k\neq 1} exp(-||y_k - y_l||^2)}$. In order to avoid having p_{ij} with extremely small values which results from outliers, p_{ij} is first set by $p_{ij} = \frac{p_{j|i} + p_{i|j}}{2n}$ so that $\sum_j p_{ij} > \frac{1}{2n}$ for all data points x_i. The gradient of symmetric SNE is computed using $\frac{\delta C}{\delta y_i} = 4\sum_j (p_{ij} - q_{ij})(y_i - y_j)$.

In t-SNE, just as discussed above, Student t-distribution with one degree of freedom will take the place of Gaussian distribution as the heavy-tailed distribution in the low-dimensional map. q_{ij} will now be computed using $q_{ij} = \frac{(1+||y_i - y_j||^2)^{-1}}{\sum_{k\neq 1}(1+||y_k - y_l||^2)^{-1}}$. A student t-distribution with one degree of freedom is used because it has the property $(1 + ||y_i - y_j||^2)^{-1}$ wherein it approaches an inverse law for large pairwise distances in the low dimensional map. The resulting map representation of joint probabilities will make the map points invariant to changes in the scale of the map. Large clusters of points that are far apart will also interact just the same way as how an individual point would.

The gradient of the Kullback-Leibler divergence between P and the Student t-based joint probability distribution Q can be computed using $\frac{\delta C}{\delta y_i} = 4\sum_j (p_{ij} - q_{ij})(y_i - y_j)(1 + ||y_i - y_j||^2)^{-1}$. The resulting gradient from t-SNE will strongly repel dissimilar data points resulting in a visual image that clearly separates each data class as can be clearly seen in the t-SNE results in Appendix E as compared with the results from the other dimensionality reduction techniques used.

In their experiment set-up, they used a total of three data sets as was discussed back in Chapter 2 which includes the MNIST data set, the Olivetti faces data set,

and the COIL-20 data set. They first used PCA to reduce the dimensionality of the data to 30 so that the computation of pairwise distances between data points would be faster and at the same time also suppresses the noise without severely distorting the distances between the data points. They then applied different dimensionality reduction techniques which includes Sammon mapping, Isomap, and LLE to compare the resulting visualization later on with the result of t-SNE. The results of each data set for each technique on the MNIST data set can be viewed in Appendix E. The coloring scheme in the visual images represent each class of data. The cost function parameter they used for their experiment was Perp = 40 for t-SNE, none for Sammon mapping, and k = 12 for Sammon mapping and Isomap.

Their results show that t-SNE overall had better visualization because the data classes are more distinct or separated than compared with the results from the other methods. In general, t-SNE outperformed all the other dimensionality reduction techniques used in their research; however, the authors point out that t-SNE has three general weakness to consider. The first one is that it is unclear how t-SNE will perform on the more general task of dimensional reduction. In other words, if dimensionality is increased to more than 3, it is unclear whether t-SNE will still produce optimal visualization results. One way of addressing this problem is to optimize the Student t-distribution to have more than one degree of freedom. The second weakness is the curse of intrinsic dimensionality since t-SNE only reduces the dimensionality of data based on the local property of the data. Data sets that have high intrinsic dimensionality and an underlying manifold that is highly varying causes the local linearity of assumption on the manifold that t-SNE implicitly makes be violated; therefore, applying t-SNE to data sets with high intrinsic dimensionality can produce unreliable results. One way to address this problem is to perform t-SNE on a data representation obtained from a model that represents the highly varying data manifold efficiently in a number of non-linear layers. The last weakness is the non-convexity of the t-SNE cost function. Since the cost function of t-SNE is non-convex, several optimization parameters would first have to be chosen. The constructed solutions would then vary depending on the optimization parameter used each time from an initial random configuration of map data point. They explicitly point out however that the same choice of parameters can be used for different visualization tasks and the result would still be of similar

3.4 Edit Distance Metric

Edit distance quantifies how dissimilar two strings are by counting the minimum number of allowable operations required to transform one string to another. There are different definitions for edit distance, each of them using a different set of single-character operations.

3.4.1 Levenshtein Distance

Given two strings, a and b over a finite alphabet, the Levenshtein distance is the minimum-weight sequence of operations that transforms a into b. In 1966, Levenshtein defines a set of three edit operations. Insertion is the insertion of a single symbol. If $X = ab$, then inserting the symbol c produces acb. Insertion can also be applied to an empty string, as denoted $\epsilon \rightarrow c$, using ϵ to denote the empty string. Deletion of a single symbol changes acb to $ab(c \rightarrow \epsilon)$. Substitution of a single symbol x for a symbol $y \neq x$ changes acb to $adb(x \rightarrow y)$. The three operations have non-negative unit costs; however, substitution of a character by itself has zero cost.

The Levenshtein distance is mathematically defined as the distance between two strings is given by $lev_{a,b}(len(a), len(b))$ where $lev_{a,b}(i, j)$ is equal to $max(i, j)$ if $min(i, j) = 0$, otherwise you take the minimum of the three operation costs. $lev_{a,b}(i, j) = max(i, j), if min(i, j) = 0; otherwise, min(lev_{a,b}(i-1, j)+1), min(lev_{a,b}(i, j-1) + 1), or\ min(lev_{a,b}(i - 1, j - 1) + 1_{a_i \neq b_j})$

The distance between the first i characters of a and the first j characters of b can be computed by using the recursive definition above. $1(ai \neq bj)$ is the indicator function equal to 0 when $ai = bj$ and equal to 1 otherwise. The first element in the minimum function corresponds to the deletion operation, the second to the insertion operation and the third to match.

Levenshtein distance has several upper and lower bounds. The distance should be at least the difference of the sizes of the two strings and at most, the length of the longer string. The distance is zero if and only if the strings are equal. Lastly, the distance between two strings is no greater than the sum of their Levenshtein distances from a third string, which satisfies the triangle inequality.

Levenshtein distance can be implemented using java-string-similarity, a Java library by tdebatty implementing different string similarity and distance measures. Here, the Levenshtein distance is computed using dynamic programming (Wagner-Fischer algorithm), which has a space requirement of $O(m)$ and runs in $O(m * n)$.

Marzal and Vidal (1993) proposed an algorithm that computes for the normalized edit distance that works in $O(m * n/sup\ 2/)$ time and $O(n/sup\ 2/)$ memory space, where m and n are the lengths of the strings under consideration, and $m >= n$. Their research shows that normalized edit distance consistently provides better results than regular edit distance and post-normalized edit distance.

The normalized Levenshtein distance is then computed with maximum alignment, dividing the Levenshtein distance by the maximum length of the two strings.

3.4.2 Damerau-Levenshtein Distance

In relation to Levenshtein distance, Damerau-Levenshtein allows another edit operation, the transposition of two adjacent characters. The Damerau-Levenshtein distance between two strings a and b is given by $d_{a,b}(i,j)$, whose value is a distance between an initial substring of string a and a j symbol prefix of b. The function is recursively defined below. $d_{a,b}(i,j) = max(i,j)\ if min(i,j) = 0$, $min(d_{a,b}(i-1,j)+1, min(d_{a,b}(i,j-1)+1), min(d_{a,b}(i-1,j-1)+1)$,or $min(d_{a,b}(i-2,j-2)+1)$ if $i,j > 1$ and $a_i = b_{j-1}$ and $a_i - 1 = b_j$; otherwise, $min(d_{a,b}(i-1.j)+1), min(d_{a,b}(i,j-1)+1)$,or $min(d_{a,b}(i-1,j-1)+1_{(a_i \neq b_j)})$.

Each recursive call matches one of the cases covered by the Damerau-Levenshtein distance. The first one corresponds to the delete operation, the second, to the insert operation, the third, to match or mismatch, depending on whether the respective symbols are the same, and the fourth, to the transposition of two adjacent symbols.

Damerau-Levenshtein can be implemented in two different ways, restricted and unrestricted. The restricted implementation is known as the Optimal String Alignment distance and the unrestricted implementation is what is commonly referred to as Damerau-Levenshtein distance.The main difference between the two implementations is that the Optimal String Alignment algorithm computes the number of edit operations under the restriction that no substring is edited more than once. Another key difference is that Optimal String Alignment algorithm is considered a true metric, since the triangle inequality does not hold, unlike the classic Damerau-Levenshtein.

The two algorithms are extensions of the Wagner-Fischer dynamic programming algorithm, which is also used in computing for the Levenshtein distance.

3.4.3 Longest Common Subsequence

Compared to the classic three-operation definition of edit distance, longest common subsequence only allows insertion and deletion. The Longest Common Subsequence (LCS) distance could also be equal to the Levenshtein distance when the cost of substitution is the double of the cost of an insertion or deletion. LCS simply gets the longest string that both string being compared to have. This can be accomplished via dynamic programming by simply appending to an initial empty string (main match) every time a match between the two strings is found. When a mismatch occurs, the loop is simply traversed without doing anything. If a succeeding match is found after the first match, a new temporary empty string is used to append the characters until a mismatch occurs. Then this temporary string will simply be compared to main match and whichever is longer will be the one stored in main match. The process is repeated until the end of both strings.

3.4.4 Difflib Python Library

Python has a built-in library called difflib which particularly provides classes and functions for sequence matching. They can be used to compare any types of sequences such as files, strings, patterns, etc. The SequenceMatcher class in difflib can be used to compare pairs of sequences of any type, as long as the elements are hashable (Python Software Foundation, 2018).

The algorithm used by the library dates back to Ratcliff and Metzener (1988)s gestalt pattern matching wherein the basic algorithm is to find the longest contiguous matching subsequence that contains no junk element. The same concept is then applied to the left and to the right of the substring until a match that looks right to people is found.

Chapter 4

Pipeline

This chapter contains procedures that propoenents will follow for the research based from theories and concepts discussed in chapter 3 and the methodologies discussed in chapter 1.

4.1 Data Collection

In this phase, the proponents expanded the original music dataset for SOMphony. Each of the 5 eras now has 5 composers with 5 symphonies each. This sums up to a total of 125 symphonies. The proponents have also decided to only include composers that have composed at least 5 symphonies to be able to maintain a balanced data set. The process of selecting which symphonies to be added would be by random to have a better grasp of the general style of the composer. The audio files were retrieved from online sources and physical means. The researchers did not take into consideration the file type and bitrate of the audio files since music data that is free for use is limited.

4.2 Data Preprocessing

The audio files were trimmed using Audacity, removing the silent parts usually found at the start and/or end of the composition. This would reduce the amount of empty data, since no features can be extracted when there is no audio. After the music files were trimmed, they will be cut into one second music segments

with a half-second overlap as discussed in Section 1.5.3 using Direct WAV MP3 Splitter.

4.3 Feature Extraction

The music segments then had their features extracted using jAudio, producing an XML file as an output. The proponents have decided to extract 436 features, refer to Appendix C for the complete list with their descriptions. All the features that dont have variable-sized dimension were the ones selected. The XML file will then be converted into CSV format. The result would be a CSV file containing all the features determined for each segment. The proponents would then run a RegEx script from SOMphony to extract the unnecessary text in preparation for labeling. The data needs to be labeled according to their composer, composition and file name.

4.4 Feature Selection

In this phase, the proponents trimmed down the 436 features that jAudio has extracted to lessen the training time for the SOM. Since a lot of features were already reduced in the jAudio step through the removal of columns with entire 0 values and columns with at least a single NaN value, this leaves a total of only 276 features with values that have actual relevant values. Principal component analysis was further used to reduce the number of features by merging columns that have similar data, until the dataset is only represented by 50 features while still retaining the essence of the original data.

4.5 t-SNE

T-SNE was performed on the processed dataset by using the tool provided by Pythons sklearn following Maaten & Hiton (2008)s concept. After which, the resulting points of one second music segment, with a total of 330777, were further processed with k-means clustering to be able to perform quantitative comparisons. Using the elbow method, it was concluded that k=5 would be the best k as shown in Figure 4.1 and after performing k-means clustering, the resulting points with their corresponding cluster label were extracted and was used to perform pairwise string comparisons for all the symphonies using different metrics. Since t-SNE

produced good results and had the same purpose as SOM, the proponents decided to focus more on t-SNE instead of SOM due to the faster processing time.

Figure 4.1: Elbow Method Result

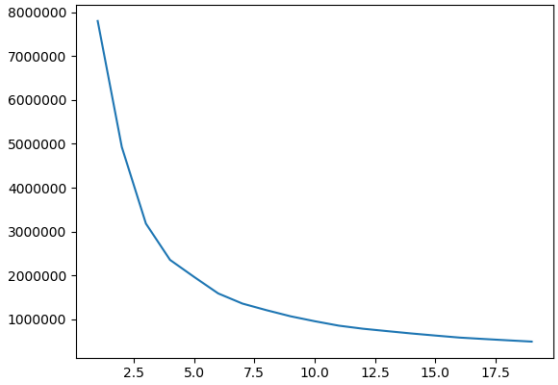

4.6 Distance Metrics

Different metrics for comparing symphonies similarities pair-wise such as Levenshtein Distance, Damerau-Levenshtein Distance, Longest Common Subsequence, Manhattan Distance were used and the results are tabulated in chapter 5 for further analysis and discussion. For each metric, the comparisons were made via two methods, one using the unchanged number of points (330777) and the other being only the transitions and this was done by compressing points with similar cluster labels and simply getting their centroid to represent the entirety of the compressed points. In this way, we can also see if simply comparing transitions would be a good enough tool for comparison compared to using the full length of points of each symphony produced by t-SNE.

As seen in Figure 4.1, the yellow and blue edges represent the trajectory of each of the symphonies as they progress through time. A line is drawn between two points from both symphonies to show the Euclidean distance between the BMUs at the particular time slice. The color of this line would change depending on the euclidean distance, which has a direct implication on the similarity of the two BMUs. Parts of the ribbon that appear to be green would signify that at these time slices, the symphonies sound similar. The parts that appear red would be the parts where the symphony will appear the least similar.

4.7 Evaluation

Frequency cluster counting will be used to determine if a pair of symphonies are alike. Each time a BMU appears inside a cluster, the frequency count for that cluster is incremented. In this way, the clusters frequently visited throughout the length of the musical piece, will have a large frequency count. The frequency counts are then normalized by dividing the counts of a certain composition by its total number of 1-second segments. Once these normalized frequency counts are summarized, the resulting percentages can then be used to perform pair-wise comparisons between symphonies.

The resulting visualization from SOM and t-SNE will then be used to verify both methods accuracy by comparing for example if two symphonies by composer A have a much similar visualization. If the resulting visualizations show that the compositions by the same composer are alike, then it may be able to prove the accuracy of the visualization technique used.

Chapter 5

Results and Analysis

This chapter contains all the results from the research conducted and the corresponding analyses for the results.

5.1 t-SNE Visualization Results

After t-SNE was applied on the dataset as was discussed in Chapter 4, the resulting points were plotted according to different categories.

5.1.1 Per Period Plot

Figure 5.1 shows the plots for different musical periods. Each of the colors represent a different composer in each period: blue for composer 1, green for composer 2, red for composer 3, purple for composer 4, and yellow for composer 5. All five periods had a similar shape of a ball since all of them represents an entire period of music and it would only be appropriate that the points are evenly scattered in the plane. Baroque period, however, has an obvious lack of plotted points in the figure compared to the others since this period in particular had the lowest number of data points originally due to the fact that the symphonies from here are generally shorter in time span. 20th Century, on the other hand, shows a more concentrated ball shape as opposed to others since this period had symphonies that are generally longer than that of other periods.

Figure 5.1: Per Period Plot

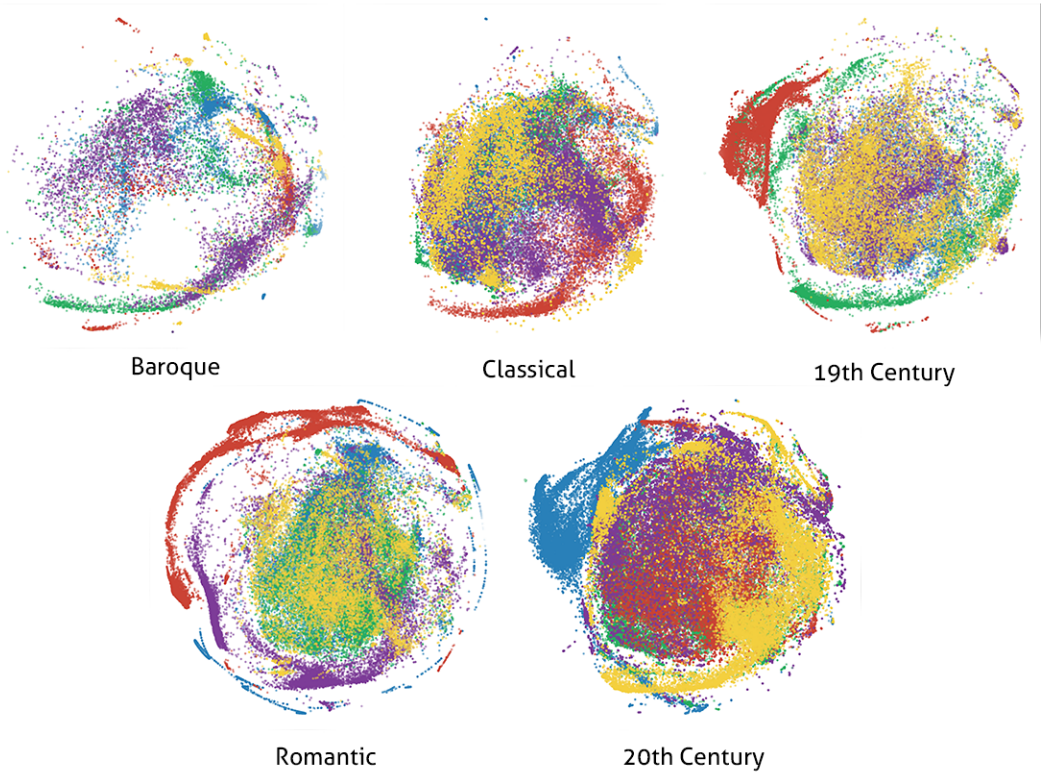

5.1.2 Per Composer Plot

Figure 5.2 shows the plots of the different composer through each period. The first row of plots are from the Baroque Period, then plots from the Classical, 19th Century, Romantic and 20th Century Periods respectively.

5.1.3 Per Symphony Plot

In order to represent the time-series aspect of the visualization, the researchers color graded the plotted points as the points aged. The colors span from yellow to green, to blue and to violet, from start to end respectively. An example of this gradation can be seen in Figure 5.3, which is the plot of (P5C2S5).

The gradation is done to all symphonies and is grouped and presented by music period. Figures 5.4 to 5.8 show the plots of each symphony as it progresses through time.

Figure 5.2: Per Composer Plot

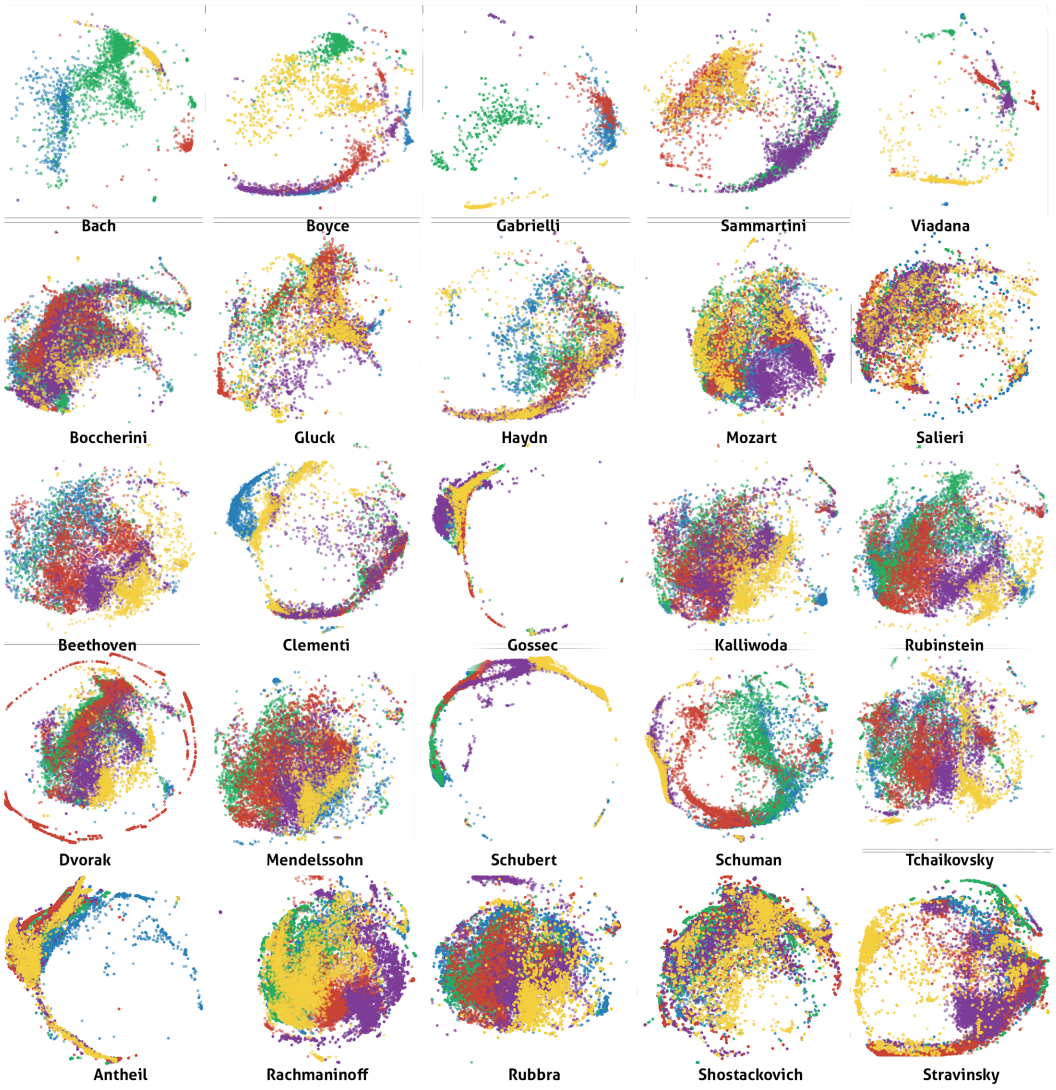

Figure 5.3: Symphony Plot

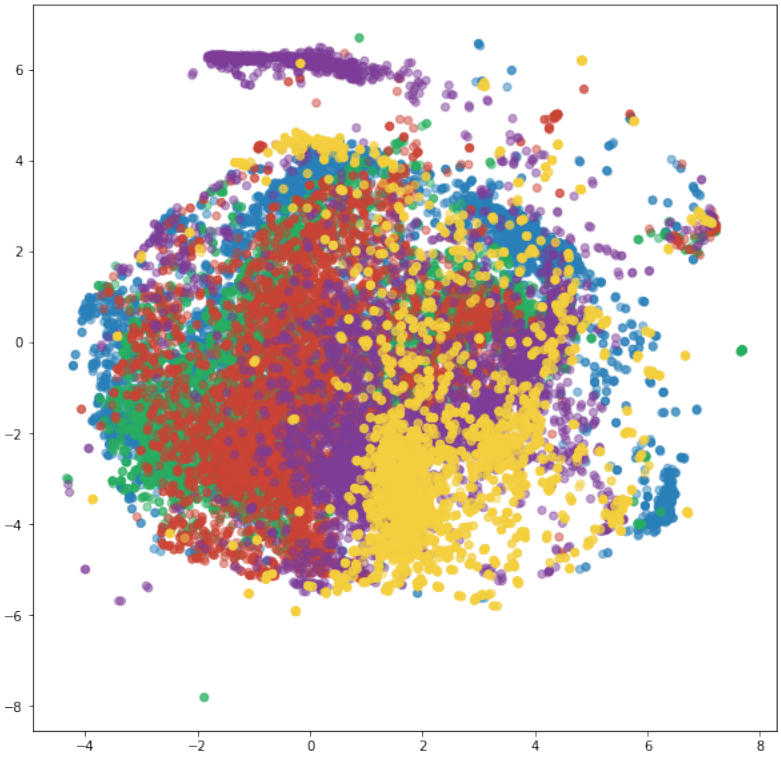

Figure 5.4: All Symphonies Part 1

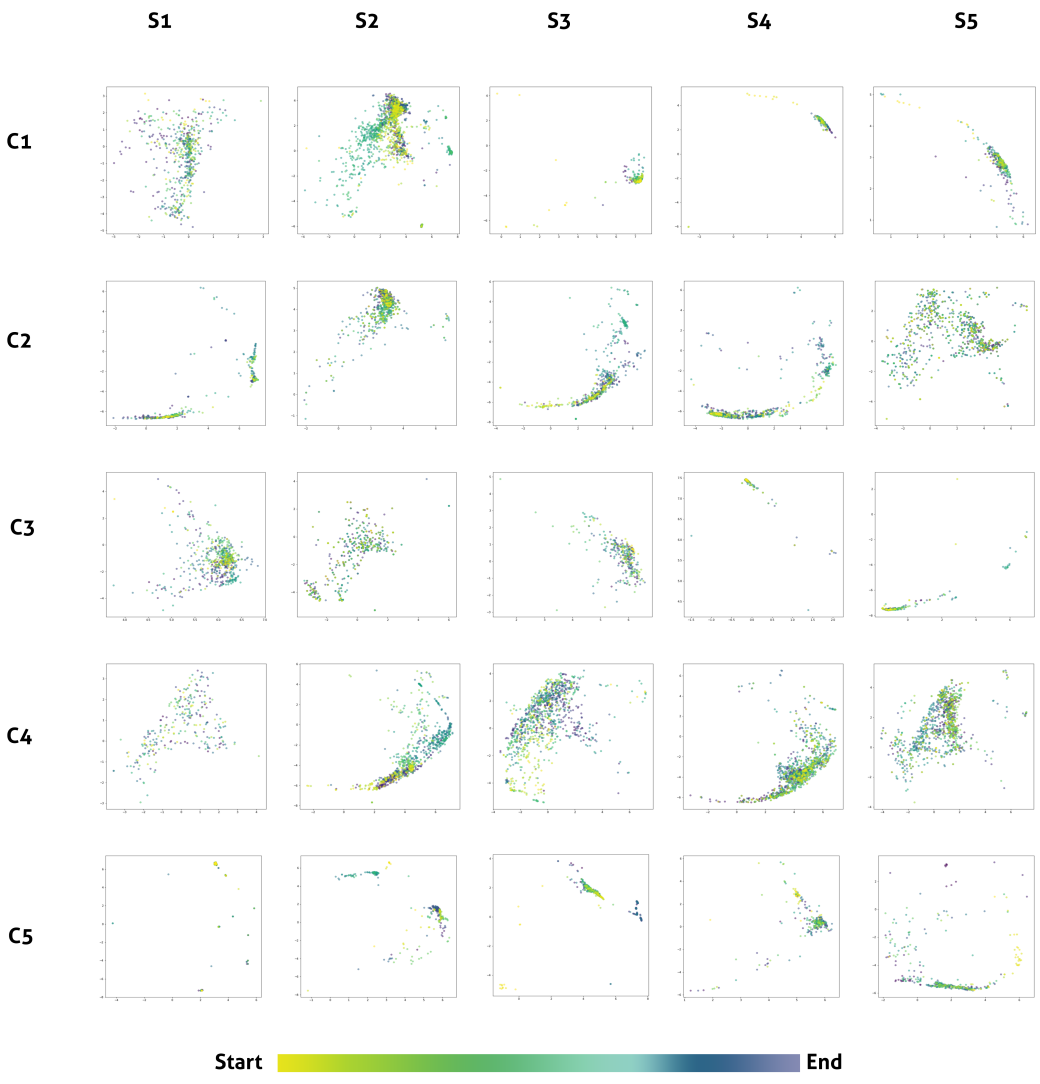

Figure 5.5: All Symphonies Part 2

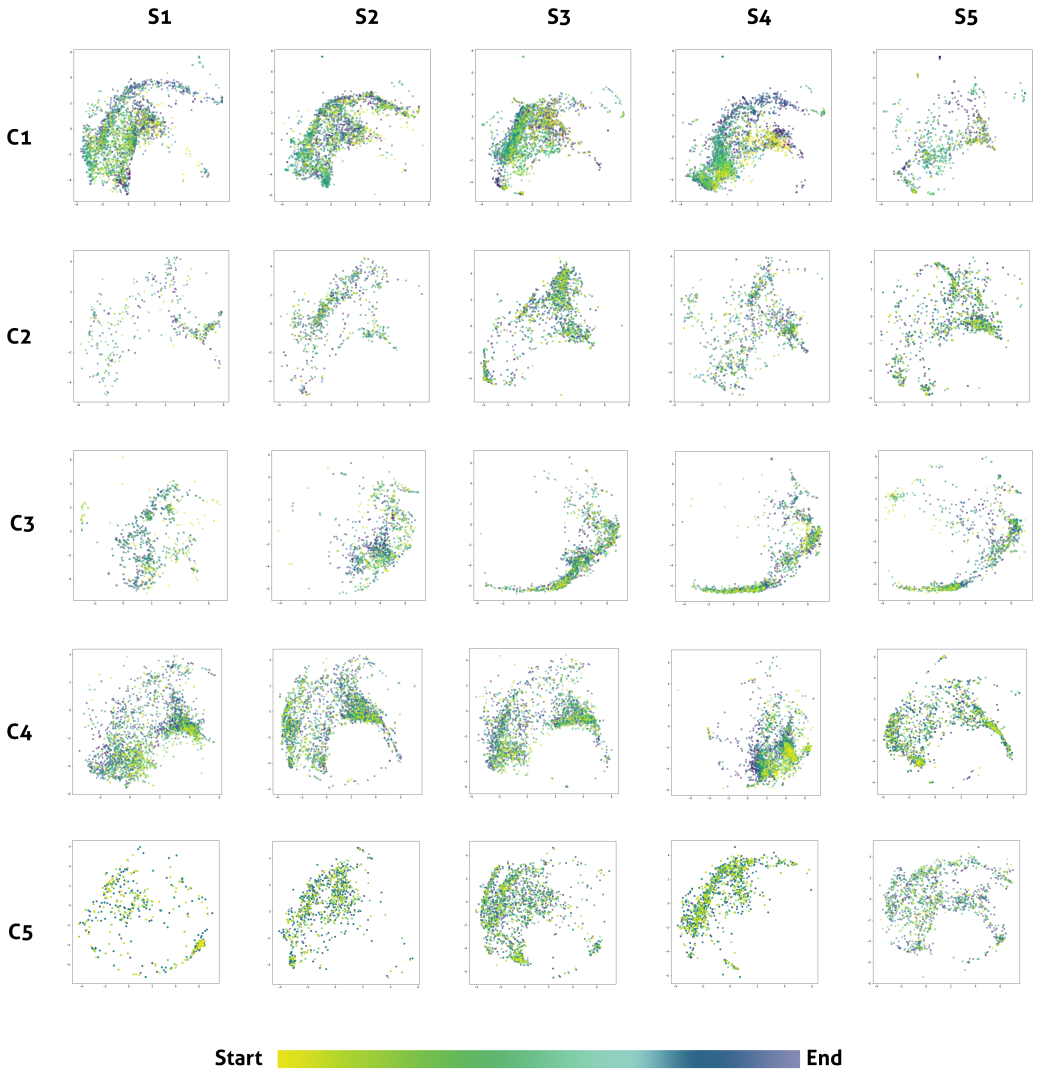

Figure 5.6: All Symphonies Part 3

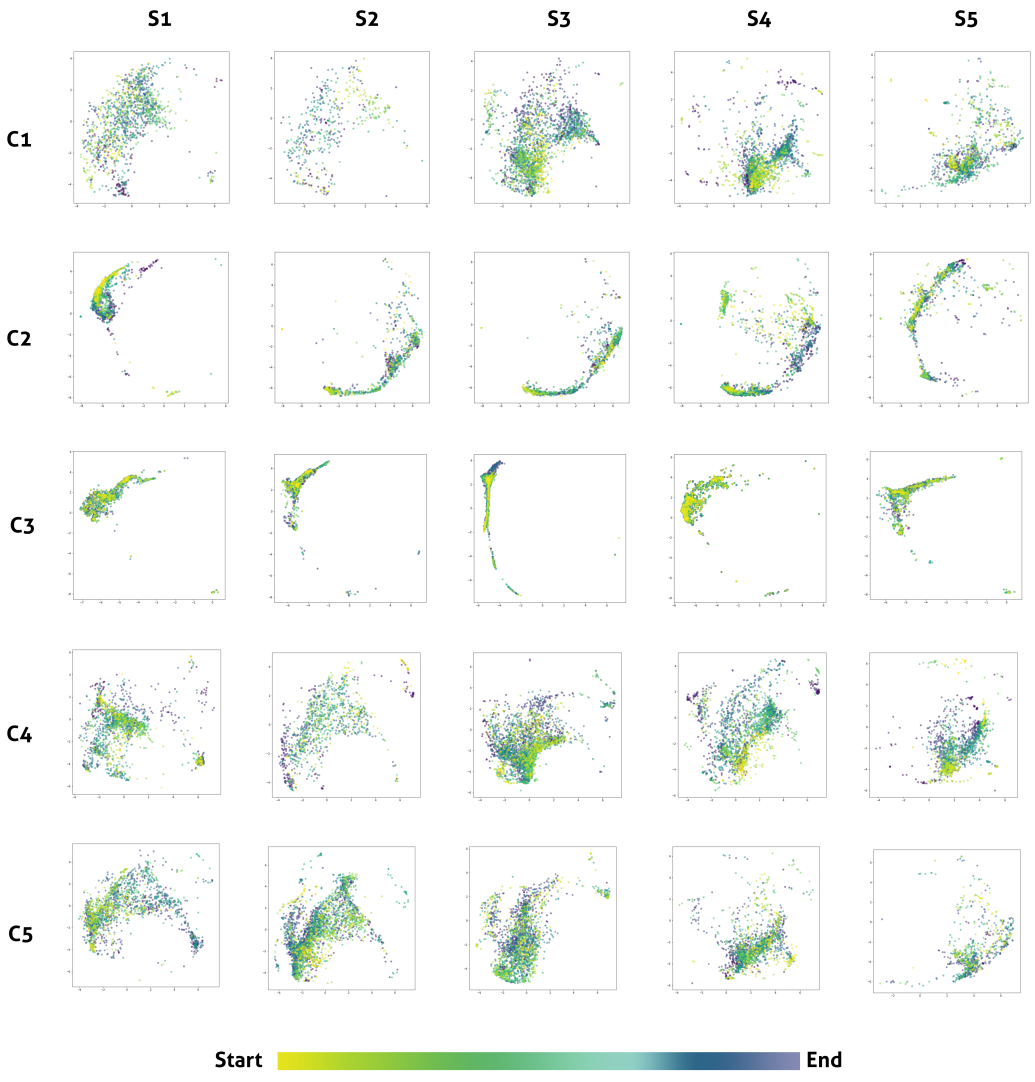

Figure 5.7: All Symphonies Part 4

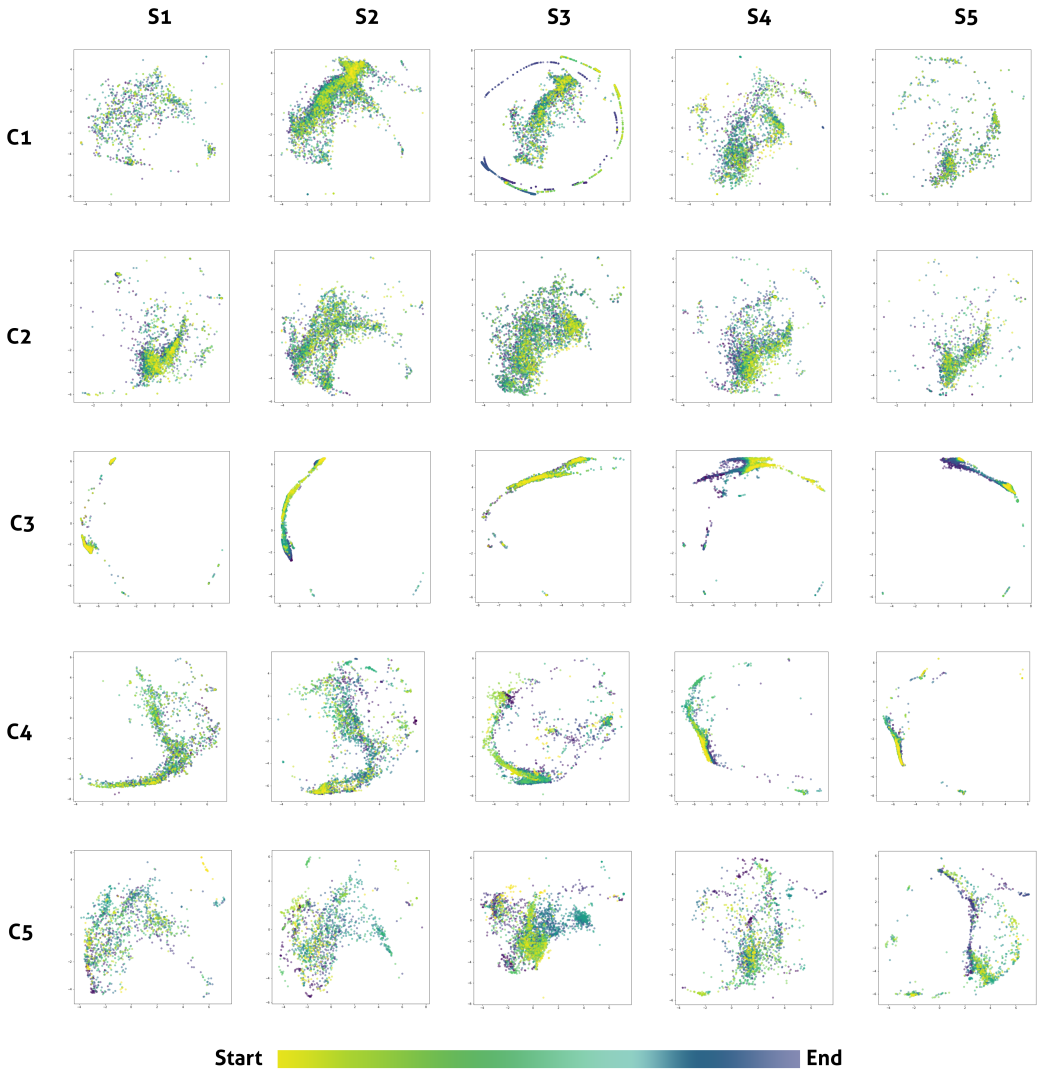

Figure 5.8: All Symphonies Part 5

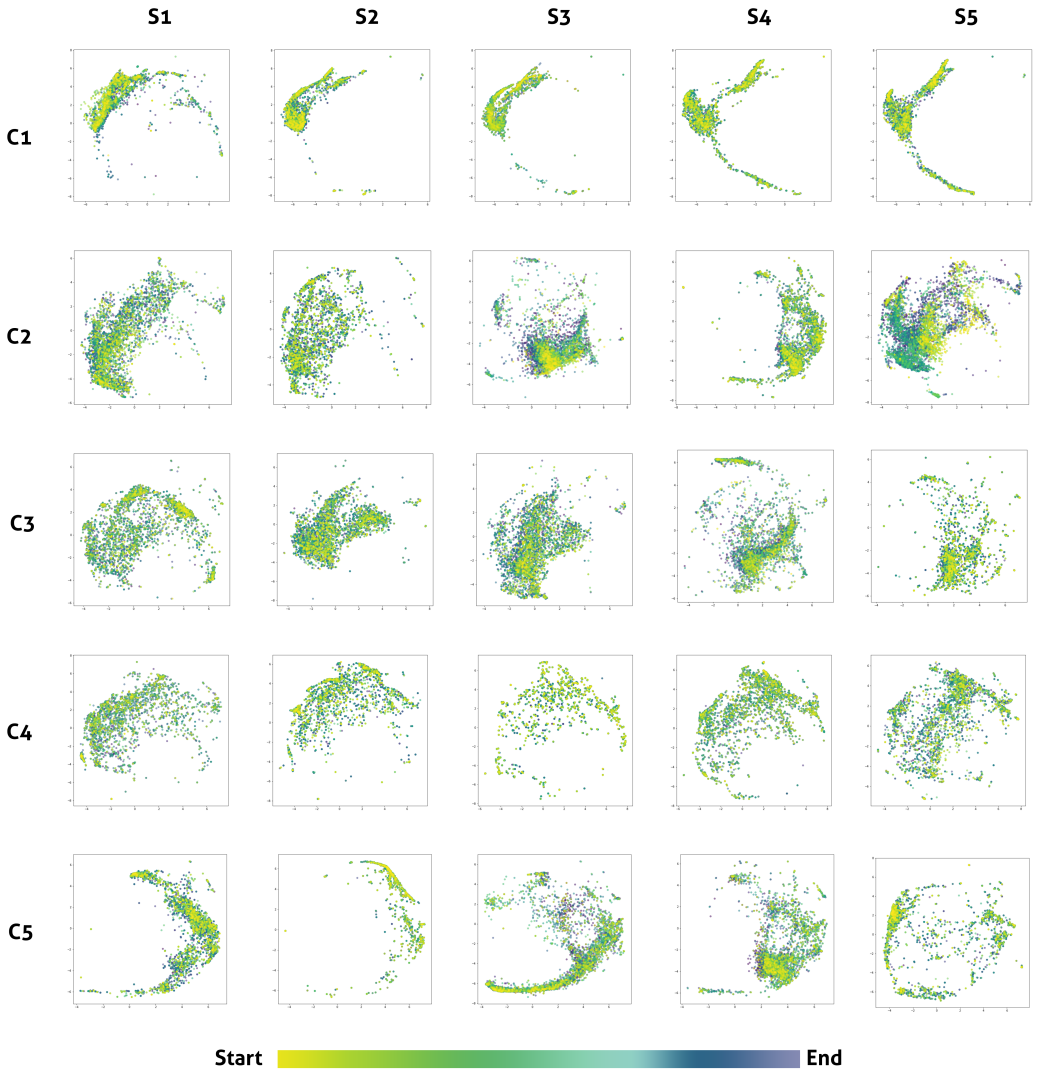

5.2 Qualitative Analysis

Based on the t-SNE results of the 5 composers in the Baroque period, the researchers noticed that the points are not that scattered and forms an arc like shape. Each composer in the Baroque period have points that are located near each other especially Boyce and Sammartini. The other 3 composers in the Baroque period are parts of the pattern that the Boyce and Sammartini produced. This result may suggest that composers in the Baroque period have similar styles of composition. In the graph of the 5 Classical composers, the points also form a similar pattern except for 1 composer, Haydn. The consistency and the solidness of the points are more noticeable in the Classical period compared to the Baroque Period. In the 19th Century Period, the results are a bit scattered throughout the map and composers Clementi and Gossec are noticeably having their own pattern. The other 3 composers of the 19th Century are the ones that created a similar pattern. This results in the 19th Century suggests that composers during this time have their own style of compositions, within the 5 composers of the 19th Century. In the Romantic Period, the graph resulted in a more diverse pattern of each composers compared to the 19th Century. There is no specific pattern or style that was shown in the graph that could determine the style of the Romantic Period composers. The same goes with the 20th Century, various styles are shown in the graph. In the earlier Periods like Baroque and Classical, more consistent and similar pattern styles are observable. This analysis suggests that early composers tend to have similar styles in composing symphonies. Through time, composers in the 19th Century, Romantic, and 20th Century period are more unique in terms of the way they compose their symphonies.

In terms of transition, the researchers noticed that the most number of similar graphs, visually looking, are present in all periods but are more dominant in the periods of Classical, 19th and 20th Century Composers. An example is the compositions of Mozart, wherein his graph has a similar pattern with 19th Century composers Beethoven, Kalliwoda and Rubinstein. This pattern continues to be present in the works of the Romantic period composers Mendelssohn and a little bit of Tchaikovsky. Lastly, the trend continues in the 20th Century composers Rachmaninoff and Rubbra. The pattern described throughout the periods is observed as a round shape style. Shown below is the development of the pattern that rooted in the composition of Mozart.

Figure 5.9: Classical: Mozart

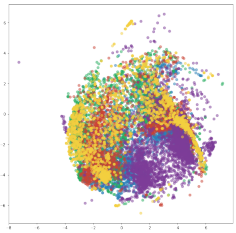

Figure 5.10: 19th Century: Kalliwoda

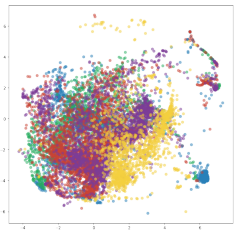

Figure 5.12: Romantic: Mendelssohn

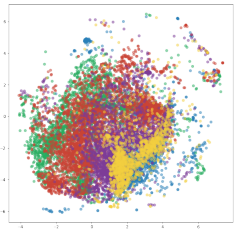

Figure 5.14: 20th Cen: Rachmaninoff

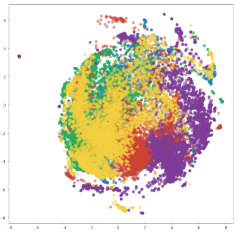

Figure 5.16: 19th Century: Rubinstein

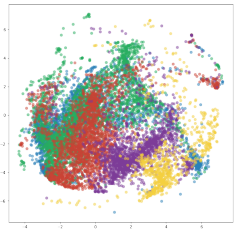

Figure 5.11: 19th Century: Beethoven

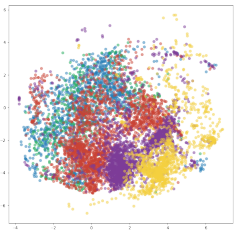

Figure 5.13: Romantic: Tchaikovsky

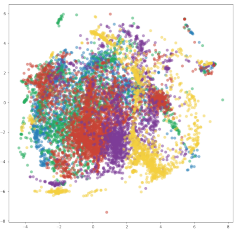

Figure 5.15: 20th Cen: Rubbra

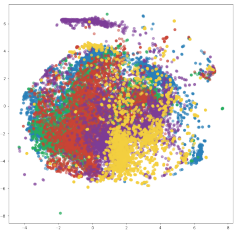

Another pattern that the researchers noticed is between the composers of the Barque, Classical and 19th Century. A unique pattern was observed to these two Baroque composers Boyce and Sammartini. Both composers have the most similar pattern in the Baroque Period as shown below.

Figure 5.17: Baroque: Boyce

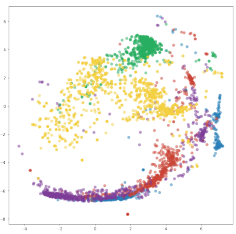

Figure 5.18: Baroque: Sammartini

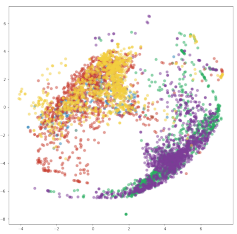

In the Classical Period, composer Haydn had the same pattern except on the top left part of the graph. The research considered that the pattern of Haydn is still relevant or influenced by the Baroque composers because the left and bottom part of the graph is similar. Two of Haydns are the ones that influence the change of the graph in comparison to the Baroque composers. The graphs of the said composers would be more similar without the two works of Haydn. Moving on to the Classical period, the trends was observe to be present in the works of Clementi. Just like Haydns, the same top left area is the main difference compared to the Baroque composers that was also caused by two of his compositions. Without the blue and yellow points of Clementi, the graph would become more similar with the other composers.

Figure 5.19: Classical: Haydn

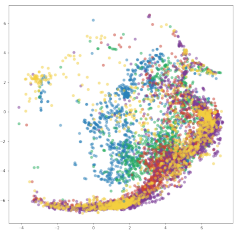

Figure 5.20: 19th Century: Clementi

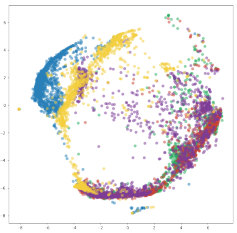

Lastly, the same pattern extended until the 20th Century with composer Stravinsky. Stravinsky has a very similar pattern with the 19th Century composers. Shown below is the graph of Stravinsky.

The results of the graphs may suggest that the works of the 19th and 20th Century composers are influenced by previous periods. The works of Boyce and Sammartini are the root of this specific style pattern that might be adapted to the next period.

Figure 5.21: 20th Cen: Stravinsky

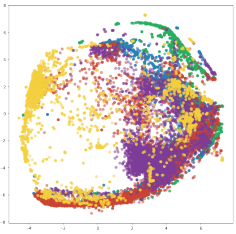

The researchers also noticed a pair of composers which had the most distinguishable pattern because the points are only located in the left side of the graph. 19th Century composer Gossec and 20th Century composer Antheil produced similar style pattern which may suggest that Antheils work is influenced by Gossec.

Figure 5.22: 19th Century: Gossec

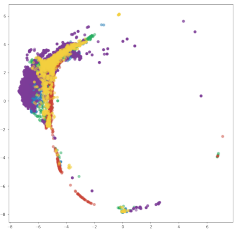

Figure 5.23: 20th Cen: Antheil

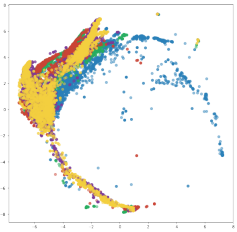

5.3 Quantitative Analysis

Table 5.1 below shows the frequency count of each cluster per symphony. Each time a point is found in a cluster, the frequency count of the corresponding label is incremented. Table 5.5 shows the percentage of the same frequency distribution table of clusters per symphony. Cluster label A has the highest number of frequency with a total of 86983, followed by B with 65867, E with 65355, D with 60726, and lastly C with 51845. These cluster counts can be used to help verify the similarity of symphonies by, for example, checking the results from the above comparisons and seeing whether their cluster counts are truly similar. Since cluster counts do not incorporate the presence of time, unlike the previous comparisons, it is highly unlikely that comparisons made would be similar.and tabulated.

Table 5.1: Frequency Cluster Count

Row Labels	A	B	C	D	E	Grand Total
P1C1S1	383	43	6	152	1	585
P1C1S2	116	1609	2	16	710	2453
P1C1S3	4	3		1	795	803
P1C1S4	2	243				245
P1C1S5	1	352		3	2	358
P1C2S1	223	14			153	390
P1C2S2	4	841	3	31	1	880
P1C2S3	106	100			431	637
P1C2S4	479	18	5	5	154	661
P1C2S5	180	415	48	291	339	1273
P1C3S1	1	41			596	638
P1C3S2	450	73	5	32	71	631
P1C3S3		90		1	227	318
P1C3S4	2	10		387		399
P1C3S5	276	2		1	23	302
P1C4S1	58	99	20	82	22	281
P1C4S2	83	109		2	783	977
P1C4S3	297	286	83	408	57	1131
P1C4S4	104	78		4	1344	1530
P1C4S5	134	690	72	253	44	1193
P1C5S1	33	952	2	1	24	1012
P1C5S2	2	241		5	87	335
P1C5S3	12	338		1	111	462
P1C5S4	7	70			251	328
P1C5S5	268	13		2	133	416

P2C1S1	1369	643	228	414	121	2775
P2C1S2	1055	827	77	398	180	2537
P2C1S3	988	686	107	806	143	2730
P2C1S4	1808	534	22	217	425	3006
P2C1S5	478	148	18	90	232	966
P2C2S1	86	91	40	40	191	448
P2C2S2	180	258	60	270	110	878
P2C2S3	336	1059	104	180	373	2052
P2C2S4	353	287	39	32	454	1165
P2C2S5	545	709	34	121	667	2076
P2C3S1	279	369	12	22	249	931
P2C3S2	72	206	2	8	804	1092
P2C3S3	259	133	1	1	1218	1612
P2C3S4	623	192	1	4	864	1684
P2C3S5	504	123	6	81	599	1313
P2C4S1	1396	330	16	44	1164	2950
P2C4S2	764	612	421	265	845	2907
P2C4S3	1082	293	71	162	913	2521
P2C4S4	881	208	30	11	2112	3242
P2C4S5	1091	546	492	271	771	3171
P2C5S1	694	521	232	703	1446	3596
P2C5S2	700	653	476	1144	80	3053
P2C5S3	1375	373	539	792	281	3360
P2C5S4	1145	1119	629	1408	26	4327
P2C5S5	472	381	129	301	339	1622
P3C1S1	514	411	87	296	46	1354
P3C1S2	246	103	14	84	28	475
P3C1S3	1460	258	65	112	498	2393
P3C1S4	1032	102	15	29	933	2111
P3C1S5	47	116	2	3	1109	1277
P3C2S1	36	3	1653	237	2	1931
P3C2S2	371	70	10	1	554	1006
P3C2S3	461	41	9		531	1042
P3C2S4	1048	102	80	199	574	2003
P3C2S5	487	73	434	444	15	1453
P3C3S1	32		1351	724		2107
P3C3S2	18		1068	598	5	1689
P3C3S3	173		1568	245	4	1990
P3C3S4	54	10	3109	1114	4	4291
P3C3S5	42		1139	521		1702

P3C4S1	1028	139	53	378	462	2060
P3C4S2	414	316	118	250	90	1188
P3C4S3	2275	340	135	192	346	3288
P3C4S4	1021	522	108	145	469	2265
P3C4S5	602	194	6	13	879	1694
P3C5S1	592	311	377	347	317	1944
P3C5S2	1493	740	244	546	101	3124
P3C5S3	1753	286	129	329	22	2519
P3C5S4	713	126	14	28	938	1819
P3C5S5	27	70	2	4	723	826
P4C1S1	429	316	106	186	143	1180
P4C1S2	820	2985	264	1919	58	6046
P4C1S3	1145	1717	357	621	307	4147
P4C1S4	1088	519	54	107	346	2114
P4C1S5	612	215	2	88	424	1341
P4C2S1	438	182	1	100	2682	3403
P4C2S2	1456	575	207	490	115	2843
P4C2S3	2016	1059	103	332	524	4034
P4C2S4	1329	354	17	46	804	2550
P4C2S5	593	94		15	848	1550
P4C3S1	15		2838	1617	21	4491
P4C3S2	7		2373	1664	8	4052
P4C3S3	46		168	5139		5353
P4C3S4	12	253	153	3404	12	3834
P4C3S5	4	3885		62	99	4050
P4C4S1	889	497		15	1337	2738
P4C4S2	1195	566	2	201	910	2874
P4C4S3	1875	66	212	287	342	2782
P4C4S4	138	1	3393	25		3557
P4C4S5	40	7	3044	60		3151
P4C5S1	379	367	243	401	70	1460
P4C5S2	673	250	204	327	140	1594
P4C5S3	1866	331	157	398	408	3160
P4C5S4	672	379	7	104	476	1638
P4C5S5	168	354	33	87	842	1484
P5C1S1	46	471	1397	3291	101	5306
P5C1S2	158	15	3637	1511		5321
P5C1S3	150	21	2394	1556		4121
P5C1S4	472	11	3292	1729		5504
P5C1S5	652	13	2826	2141		5632

P5C2S1	2968	1071	756	822	75	5692
P5C2S2	2594	683	1211	1497	157	6142
P5C2S3	2612	217	63	201	1489	4582
P5C2S4	341	1070	94	114	4240	5859
P5C2S5	3811	854	690	526	385	3199
P5C3S1	1194	1907	618	1215	493	5427
P5C3S2	2590	1264	417	734	564	5569
P5C3S3	2975	1009	212	786	419	5401
P5C3S4	1460	534	20	730	1418	4162
P5C3S5	2023	707	8	299	2572	5609
P5C4S1	585	1076	911	1186	165	3923
P5C4S2	292	1955	1144	1943	111	5445
P5C4S3	624	2737	428	1329	552	5670
P5C4S4	641	2713	719	1160	286	5519
P5C4S5	1242	2513	299	561	424	5039
P5C5S1	234	2447	6	360	3036	6083
P5C5S2	58	3071	22	26	938	4115
P5C5S3	2613	665	8	333	2554	6173
P5C5S4	251	762		170	4067	5250
P5C5S5	793	745	913	2509	777	5737
Grand Total	86983	65867	51845	60726	65355	330776

Table 5.2: Percentage Cluster Count

Row Labels	A	B	C	D	E
P1C1S1	65%	7%	1%	26%	0%
P1C1S2	5%	66%	0%	1%	29%
P1C1S3	0%	0%	0%	0%	99%
P1C1S4	1%	99%	0%	0%	0%
P1C1S5	0%	98%	0%	1%	1%
P1C2S1	57%	4%	0%	0%	39%
P1C2S2	0%	96%	0%	4%	0%
P1C2S3	17%	16%	0%	0%	68%
P1C2S4	72%	3%	1%	1%	23%
P1C2S5	14%	33%	4%	23%	27%
P1C3S1	0%	6%	0%	0%	93%
P1C3S2	71%	12%	1%	5%	11%
P1C3S3	0%	28%	0%	0%	71%
P1C3S4	1%	3%	0%	97%	0%
P1C3S5	91%	1%	0%	0%	8%

P1C4S1	21%	35%	7%	29%	8%
P1C4S2	8%	11%	0%	0%	80%
P1C4S3	26%	25%	7%	36%	5%
P1C4S4	7%	5%	0%	0%	88%
P1C4S5	11%	58%	6%	21%	4%
P1C5S1	3%	94%	0%	0%	2%
P1C5S2	1%	72%	0%	1%	26%
P1C5S3	3%	73%	0%	0%	24%
P1C5S4	2%	21%	0%	0%	77%
P1C5S5	64%	3%	0%	0%	32%
P2C1S1	49%	23%	8%	15%	4%
P2C1S2	42%	33%	3%	16%	7%
P2C1S3	36%	25%	4%	30%	5%
P2C1S4	60%	18%	1%	7%	14%
P2C1S5	49%	15%	2%	9%	24%
P2C2S1	19%	20%	9%	9%	43%
P2C2S2	21%	29%	7%	31%	13%
P2C2S3	16%	52%	5%	9%	18%
P2C2S4	30%	25%	3%	3%	39%
P2C2S5	26%	34%	2%	6%	32%
P2C3S1	30%	40%	1%	2%	27%
P2C3S2	7%	19%	0%	1%	74%
P2C3S3	16%	8%	0%	0%	76%
P2C3S4	37%	11%	0%	0%	51%
P2C3S5	38%	9%	0%	6%	46%
P2C4S1	47%	11%	1%	1%	39%
P2C4S2	26%	21%	14%	9%	29%
P2C4S3	43%	12%	3%	6%	36%
P2C4S4	27%	6%	1%	0%	65%
P2C4S5	34%	17%	16%	9%	24%
P2C5S1	19%	14%	6%	20%	40%
P2C5S2	23%	21%	16%	37%	3%
P2C5S3	41%	11%	16%	24%	8%
P2C5S4	26%	26%	15%	33%	1%
P2C5S5	29%	23%	8%	19%	21%
P3C1S1	38%	30%	6%	22%	3%
P3C1S2	52%	22%	3%	18%	6%
P3C1S3	61%	11%	3%	5%	21%
P3C1S4	49%	5%	1%	1%	44%
P3C1S5	4%	9%	0%	0%	87%

P3C2S1	2%	0%	86%	12%	0%
P3C2S2	37%	7%	1%	0%	55%
P3C2S3	44%	4%	1%	0%	51%
P3C2S4	52%	5%	4%	10%	29%
P3C2S5	34%	5%	30%	31%	1%
P3C3S1	2%	0%	64%	34%	0%
P3C3S2	1%	0%	63%	35%	0%
P3C3S3	9%	0%	79%	12%	0%
P3C3S4	1%	0%	72%	26%	0%
P3C3S5	2%	0%	67%	31%	0%
P3C4S1	50%	7%	3%	18%	22%
P3C4S2	35%	27%	10%	21%	8%
P3C4S3	69%	10%	4%	6%	11%
P3C4S4	45%	23%	5%	6%	21%
P3C4S5	36%	11%	0%	1%	52%
P3C5S1	30%	16%	19%	18%	16%
P3C5S2	48%	24%	8%	17%	3%
P3C5S3	70%	11%	5%	13%	1%
P3C5S4	39%	7%	1%	2%	52%
P3C5S5	3%	8%	0%	0%	88%
P4C1S1	36%	27%	9%	16%	12%
P4C1S2	14%	49%	4%	32%	1%
P4C1S3	28%	41%	9%	15%	7%
P4C1S4	51%	25%	3%	5%	16%
P4C1S5	46%	16%	0%	7%	32%
P4C2S1	13%	5%	0%	3%	79%
P4C2S2	51%	20%	7%	17%	4%
P4C2S3	50%	26%	3%	8%	13%
P4C2S4	52%	14%	1%	2%	32%
P4C2S5	38%	6%	0%	1%	55%
P4C3S1	0%	0%	63%	36%	0%
P4C3S2	0%	0%	59%	41%	0%
P4C3S3	1%	0%	3%	96%	0%
P4C3S4	0%	7%	4%	89%	0%
P4C3S5	0%	96%	0%	2%	2%
P4C4S1	32%	18%	0%	1%	49%
P4C4S2	42%	20%	0%	7%	32%
P4C4S3	67%	2%	8%	10%	12%
P4C4S4	4%	0%	95%	1%	0%
P4C4S5	1%	0%	97%	2%	0%

P4C5S1	26%	25%	17%	27%	5%
P4C5S2	42%	16%	13%	21%	9%
P4C5S3	59%	10%	5%	13%	13%
P4C5S4	41%	23%	0%	6%	29%
P4C5S5	11%	24%	2%	6%	57%
P5C1S1	1%	9%	26%	62%	2%
P5C1S2	3%	0%	68%	28%	0%
P5C1S3	4%	1%	58%	38%	0%
P5C1S4	9%	0%	60%	31%	0%
P5C1S5	12%	0%	50%	38%	0%
P5C2S1	52%	19%	13%	14%	1%
P5C2S2	42%	11%	20%	24%	3%
P5C2S3	57%	5%	1%	4%	32%
P5C2S4	6%	18%	2%	2%	72%
P5C2S5	119%	27%	22%	16%	12%
P5C3S1	22%	35%	11%	22%	9%
P5C3S2	47%	23%	7%	13%	10%
P5C3S3	55%	19%	4%	15%	8%
P5C3S4	35%	13%	0%	18%	34%
P5C3S5	36%	13%	0%	5%	46%
P5C4S1	15%	27%	23%	30%	4%
P5C4S2	5%	36%	21%	36%	2%
P5C4S3	11%	48%	8%	23%	10%
P5C4S4	12%	49%	13%	21%	5%
P5C4S5	25%	50%	6%	11%	8%
P5C5S1	4%	40%	0%	6%	50%
P5C5S2	1%	75%	1%	1%	23%
P5C5S3	42%	11%	0%	5%	41%
P5C5S4	5%	15%	0%	3%	77%
P5C5S5	14%	13%	16%	44%	14%

Listed below in table 5.3 are the results of using Manhattan distance for pairwise comparison of symphonies with respect to the time dimension of each symphonies. Each point in time of the t-SNE result for a symphony is matched with a point of another symphony and the distance between these two points is computed. The process is simply repeated until the end of either symphony is reached. Truncation is thus performed on the longer string to match the lengths of the two symphonies being compared. The resulting collection of distances are thus summed

The results show that Bachs sinfonia no. 7 and sinfonia no. 4 are the most similar among the entire list of symphonies, followed by Gabrielis canzon noni toni a 12-correggio with Viadanas sinfonia la bolognese, and so on. Contrary to expectation that symphonies from the same composer would be more similar compared to those of other composers, a lot of entries in the top 30 have symphonies that come from different composers. Interestingly, a lot of entries in the top 30 also come from Bachs sinfonia no. 7, which could very well indicate that its points may be well scattered throughout the map when plotted or the points could be positioned near the center of the map. Verifying this, we look at Bachs graph in Figure 5.6 and the green points, which represent Bachs sinfonia no. 7 are somewhat located near the middle of the graph. They are not, however, scattered throughout the map. Viadanas Sinfonia la Bergamasca is the second most number of matches in the top 30 and based on its graph in Figure 5.10, it can be seen that this symphony is somewhat scattered but the main bulk of its points are still near the middle. Seeing this result may well indicate that symphonies located near the middle when graphed may have a stronger tendency to have higher matches with more symphonies when comparing through distances of points via time. To furr verify this method of comparison between symphonies, we shall compare these results with the results of other metrics later on. The results of this metric together with other succeeding partial results below can be further viewed in their respective spreadsheet files as the results of these pairwise comparisons have a total number of 125x125 rows.

Table 5.3: Manhattan Distance Top Results: Full Length Summed

Symphony A	Symphony B	Distance Sum
P1C1S4	P1C1S5	269.9242
P1C3S3	P1C5S4	598.8077
P1C1S4	P1C5S3	776.0105
P1C1S4	P1C3S3	787.6107
P1C1S4	P1C5S4	807.6517
P1C4S1	P1C4S3	947.415
P1C3S3	P1C5S3	967.2533
P1C1S5	P1C5S3	970.1439
P1C4S1	P1C4S5	993.4798
P1C1S4	P5C5S2	999.3968
P1C4S1	P4C1S2A	1010.578
P1C1S4	P1C2S2	1017.719
P1C1S4	P1C5S2	1027.048
P1C4S1	P5C3S3A	1034.093
P1C4S1	P2C5S2A	1045.884
P1C4S1	P2C2S2A	1059.302

P1C4S1	P2C5S4A	1074.551
P1C4S1	P4C1S3A	1104.918
P1C4S1	P3C5S3	1117.526
P1C4S1	P4C2S3A	1130.082
P1C4S1	P3C1S1	1153.61
P1C4S1	P2C1S3	1156.801
P1C4S1	P3C1S2	1158.137
P1C1S4	P1C2S5	1167.234
P1C4S1	P4C1S4	1181.949
P1C4S1	P2C1S2	1186.405
P1C4S1	P3C5S2	1198.531
P1C1S4	P1C3S1	1222.162
P1C4S1	P2C3S1A	1225.814
P1C4S1	P2C1S1	1234.873
P1C4S1	P4C1S1A	1238.681

Table 5.4 below shows the Manhattan distance comparison of symphonies, but this time, through the transitions only. Interestingly, a lot of the rankings of the results matched that of the earlier comparisons like for example, a lot of the top 30 results here still showed Bachs sinfonia no. 7.

Table 5.4: Manhattan Distance Result: Transitions Summed

Symphony A	Symphony B	Distance Sum
P2C1S3	P1C1S4	6.342487
P2C5S3A	P1C1S4	7.09482
P3C1S3	P1C1S4	7.191891
P2C4S2A	P1C1S4	7.276127
P1C1S4	P1C1S5	7.354168
P4C2S1A	P1C1S4	7.489208
P1C2S5	P1C1S4	7.49975
P2C3S1A	P1C1S4	7.522169
P1C1S5	P1C1S4	7.667543
P1C1S4	P1C5S5	7.682119
P1C1S4	P2C3S2A	7.769781
P2C3S2A	P1C1S4	7.805628
P2C1S4	P1C1S4	7.806015
P2C2S5A	P1C1S4	7.961077
P2C3S3A	P1C1S4	7.981119
P5C2S3	P1C1S4	8.046022

P1C2S3	P1C2S3	8.079905
P4C1S1A	P1C1S4	8.13656
P4C1S5A	P1C1S4	8.149289
P2C4S1A	P1C1S4	8.167969
P2C2S1	P1C1S4	8.23078
P4C5S4	P1C1S4	8.290154
P2C5S1A	P1C1S4	8.318904
P5C5S4	P1C1S4	8.383004
P1C1S4	P2C5S1A	8.563907
P1C1S4	P1C1S2	8.621842
P1C1S4	P5C3S1A	8.723814
P1C4S5	P1C1S4	8.732073
P4C4S2	P1C1S4	8.783347
P1C1S4	P3C1S5	8.82796

If we take the the top results from the Manhattan distance above, with Bachs sinfonia no. 7 (P1C1S4) and sinfonia no. 4 (P1C1S5) being the top for Manhattan distance comparison, we can see below in Table 5.4 that indeed their cluster couts are somewhat similar with the majority of the points being in cluster B. Sinfonia no. 7 has 99% of points in B while sinfonia no. 4 has 98% of points in B. The second closest with the Manhattan result, Gabrielis canzon noni toni a 12-correggio (P1C3S3) and Viadanas sinfonia la bolognese (P1C5S4), again show the same result with their cluster counts being very similar in that both of them had near 75% of points in cluster E and nea 25% in cluster B.

Bachs sinfonia no. 7 (P1C1S4) which produced a lot of high matches with other symphonies is also coincidentally the shortest symphony among the dataset and this may indicate that truncation indeed is not a reliable method of matching the lengths of the symphonies for comparison or it could also mean that sinfonia no. 7 simply has a lot in common with most symphonies. In order to further verify this, we repeat the Manhattan distance comparison, but this time, by taking the average of the distances of all the points that were compared instead of simply adding them all up. Table 5.5 below shows the top 30 results. Bachs sinfonia no. 7 can still be seen in some entries but the entries this time around have more variance in them unlike the total distance from before.

Table 5.5: Manhattan Distance Result: Distances Mean

Symphony A	Symphony B	Distance Mean
P1C1S4	P1C1S5	1.106247
P1C3S3	P1C5S4	1.888983

P3C3S2	P3C3S5	2.709862
P1C1S5	P1C5S3	2.71749
P4C4S4	P4C4S5	2.783062
P3C2S1	P3C3S1	2.885411
P3C3S1	P3C3S2	2.894063
P1C3S3	P1C5S3	3.051272
P3C2S1	P3C3S4	3.158728
P1C1S4	P1C5S3	3.180371
P3C3S1	P3C3S3	3.197033
P3C3S2	P3C3S3	3.213563
P1C1S4	P1C3S3	3.227913
P3C3S1	P3C3S4	3.303385
P1C1S4	P1C5S4	3.310048
P1C1S1	P3C5S3	3.356575
P1C4S1	P1C4S3	3.383625
P3C2S1	P3C3S2	3.384755
P3C1S4	P4C2S1A	3.422252
P1C1S1	P1C3S2	3.433787
P2C4S4A	P4C2S1A	3.438686
P1C1S1	P3C1S1	3.472338
P3C1S4	P3C5S4	3.541771
P3C4S5	P4C2S1A	3.548003
P1C4S1	P1C4S5	3.548142
P1C5S1	P4C3S5	3.583475
P3C5S4	P4C2S1A	3.58519
P3C2S1	P3C3S3	3.594948
P1C4S1	P4C1S2A	3.609206
P2C4S4A	P3C1S4	3.637364
P1C1S1	P4C5S2	3.6608

Table 5.6 below shows the top results when longest common subsequence (LCS) is used and the symphony points were truncated to match each pair of symphonies. Table 5.7 shows the top results when LCS was used and no truncation was done. When truncation was done, a lot of top results became perfect matches as seen below and due to this, the results are deemed bad and inappropriate for comparison. The untruncated version shows better results with the top match being 61%. Table 5.8, on the other hand, shows LCS results using the transitions only. This resulted in overall lower percentage matches but may still be a good metric and shall be evaluated further later on.

Table 5.6: LCS Truncated Result

Symphony A	Symphony B	Percent Match
P1C1S3	P1C4S4	100%
P1C1S3	P2C3S4A	100%
P1C1S3	P2C4S1A	100%
P1C1S3	P2C4S2A	100%
P1C1S3	P2C4S3A	100%
P1C1S3	P2C4S4A	100%
P1C1S3	P2C5S1A	100%
P1C1S3	P3C1S4	100%
P1C1S3	P3C1S5	100%
P1C1S3	P4C2S1A	100%
P1C1S3	P4C4S1	100%
P1C1S3	P4C4S2	100%
P1C1S3	P5C2S3	100%
P1C1S3	P5C2S4A	100%
P1C1S3	P5C3S4	100%
P1C1S3	P5C3S5A	100%
P1C1S3	P5C5S1A	100%
P1C1S3	P5C5S3	100%
P1C1S3	P5C5S4	100%
P1C1S4	P1C1S2	100%
P1C1S4	P1C2S5	100%
P1C1S4	P1C4S3	100%
P1C1S4	P1C4S5	100%
P1C1S4	P1C5S1	100%
P1C1S4	P2C1S1	100%
P1C1S4	P2C1S2	100%
P1C1S4	P2C1S3	100%
P1C1S4	P2C1S4	100%
P1C1S4	P2C2S2A	100%
P1C1S4	P2C2S3A	100%

Table 5.7: LCS Full Length Result

Symphony A	Symphony B	Percent Match
P2C4S4A	P2C4S4A	61%
P2C5S2A	P2C5S2A	58%
P2C5S4A	P5C2S2A	56%
P2C4S1A	P2C4S1A	56%

P2C4S4A	P5C3S5A	55%
P2C5S4A	P5C4S2A	54%
P2C4S4A	P5C5S3	53%
P2C5S4A	P5C4S3A	53%
P2C5S4A	P5C5S5A	51%
P2C5S4A	P5C2S1A	51%
P2C5S4A	P5C4S4A	49%
P2C5S3A	P5C2S2A	49%
P2C4S1A	P5C5S3	49%
P2C5S1A	P5C3S5A	49%
P2C5S4A	P5C3S1A	49%
P2C4S4A	P5C2S4A	48%
P2C5S4A	P5C3S2A	48%
P2C4S4A	P5C5S4	47%
P2C1S4	P5C5S3	47%
P2C4S4A	P5C5S1A	47%
P2C5S4A	P5C3S3A	47%
P2C4S4A	P4C2S1A	46%
P2C1S4	P5C3S3A	46%
P2C5S4A	P5C4S5A	46%
P2C1S4	P5C2S5A	46%
P2C5S3A	P5C2S1A	46%
P2C1S4	P5C3S2A	45%
P2C1S4	P5C2S1A	45%
P2C5S4A	P5C4S1A	45%
P2C5S2A	P5C2S2A	45%

Table 5.8: LCS Transitions Result

Symphony A	Symphony B	Percentage Match
P2C5S4A	P5C2S2A	42%
P5C5S5A	P5C2S2A	41%
P5C4S3A	P5C5S5A	41%
P5C5S5A	P5C4S3A	41%
P5C2S1A	P5C2S2A	41%
P2C5S4A	P5C4S3A	41%
P5C4S2A	P5C5S5A	40%
P5C2S2A	P5C4S2A	40%
P5C2S2A	P5C4S3A	40%
P5C4S3A	P5C4S4A	40%

P2C5S4A	P5C4S2A	40%
P5C3S1A	P5C4S3A	39%
P5C2S2A	P5C3S2A	39%
P5C4S2A	P5C4S4A	38%
P5C4S3A	P5C5S1A	38%
P2C5S4A	P5C5S5A	38%
P5C3S2A	P5C4S3A	37%
P5C3S5A	P5C5S1A	37%
P2C5S4A	P5C2S1A	37%
P5C4S3A	P5C4S5A	37%
P5C1S4A	P5C1S5A	37%
P2C5S4A	P5C4S4A	36%
P5C3S5A	P5C5S3	36%
P5C2S2A	P5C3S1A	36%
P5C4S4A	P5C5S5A	36%
P5C1S5A	P5C2S2A	36%
P5C2S2A	P5C4S4A	36%
P2C5S4A	P5C3S2A	36%
P2C5S4A	P5C3S1A	35%
P5C2S1A	P5C4S3A	35%

Table 5.9 below shows the top results for sequence matcher as was discussed in Chapter 4.

Table 5.9: Sequence Match Result

Symphony A	Symphony B	Percentage Match
P1C3S1	P1C5S2	83%
P1C5S5	P3C2S3	76%
P1C5S2	P1C5S4	74%
P1C2S3	P1C2S4	72%
P4C3S2	P3C2S1	69%
P1C4S2	P1C4S4	68%
P1C2S4	P3C2S2	68%
P1C3S1	P1C3S3	67%
P3C2S2	P1C2S4	67%
P1C3S1	P1C5S4	64%
P3C3S2	P3C2S1	63%
P1C5S3	P1C5S4	63%
P1C5S5	P3C2S2	62%

P1C3S5	P1C5S5	61%
P1C2S1	P1C5S5	61%
P1C2S4	P1C5S5	60%
P1C2S4	P1C2S1	60%
P1C3S1	P1C5S3	59%
P1C2S1	P1C2S4	59%
P3C1S5	P3C2S2	59%
P3C4S5	P1C4S2	59%
P1C5S1	P3C5S5	58%
P3C2S3	P1C4S2	58%
P3C4S5	P1C4S4	58%
P3C2S3	P3C5S5	57%
P3C2S2	P3C1S5	57%
P3C3S5	P3C2S1	57%
P3C2S2	P1C5S5	57%
P1C5S2	P1C5S3	57%
P4C3S3	P3C2S1	57%

Levenshtein distance was applied to the cluster trajectories of the each symphony. Given the trajectory of the symphony, which is represented by letters from A to E, the researchers compared all of the symphonies and tabulated their respective Levenshtein distances. The same is done to the compressed version of these trajectories. Table 5.10 shows the results of Levenshtein using the full length data while 5.11 shows the transitions results.

Table 5.10: Levenshtein Result - Full Length

Symphony A	Symphony B	Distance
P1C1S4	P1C5S2	95
P1C3S3	P1C5S4	102
P1C1S3	P3C5S5	107
P1C1S5	P1C5S2	114
P1C1S4	P1C1S5	115
P1C1S5	P1C5S3	125
P1C2S1	P1C3S5	147
P1C3S5	P1C5S5	155
P1C2S2	P1C5S1	167
P1C1S4	P1C4S1	180
P1C2S1	P1C5S5	184
P1C3S3	P1C5S2	188

P1C1S3	P1C4S2	194
P1C5S2	P1C5S4	202
P1C1S3	P1C3S1	205
P1C5S2	P1C5S3	205
P1C3S1	P3C5S5	207
P1C2S3	P1C3S1	217
P1C1S4	P1C5S3	219
P1C3S5	P3C1S2	223
P1C4S1	P1C5S2	226
P1C1S4	P1C3S3	228
P1C2S1	P1C5S4	234
P1C3S3	P2C2S1	234
P1C3S5	P1C4S1	238
P1C2S4	P1C3S2	240
P1C3S3	P1C4S1	242
P1C4S2	P3C5S5	244
P1C5S4	P2C2S1	249
P1C2S1	P1C3S3	252

Table 5.11: Levenshtein Transitions Result

Symphony A	Symphony B	Distance
P1C1S3	P1C1S5	6
P1C1S5	P1C3S4	6
P1C1S3	P1C1S4	8
P1C1S4	P1C1S5	8
P1C3S1	P1C5S4	8
P1C1S3	P1C3S4	11
P1C1S4	P1C3S4	12
P1C3S1	P1C5S2	12
P1C3S5	P1C5S3	14
P1C1S5	P1C5S3	15
P1C2S1	P1C5S5	15
P1C3S4	P1C5S3	15
P1C5S2	P1C5S4	15
P1C1S3	P1C5S3	16
P1C1S3	P1C3S5	17
P1C1S4	P1C5S3	20
P1C3S1	P1C5S3	21
P1C1S5	P1C3S5	22

P1C2S1	P1C2S3	22
P1C5S3	P1C5S4	22
P1C1S4	P1C3S5	23
P1C3S4	P1C3S5	24
P1C2S1	P3C2S3	25
P1C2S3	P3C2S3	25
P1C3S5	P1C5S4	25
P1C2S2	P1C5S2	27
P1C2S3	P1C2S4	27
P1C5S5	P3C2S3	27
P1C3S1	P1C3S5	28
P1C5S2	P1C5S5	28

In order to verify which metric was the best, we compare the top 30 most similar pairs of symphonies generated by each metric and find out which two metrics had the most matches. Note also that we chose to include different implementations for each algorithm like the mean procedure of Manhattan distance over the summation procedure. Based on Table 5.12 below, mean and summation procedure of Manhattan distance would produce non-similar results since only 10 out of 30 matched.

Among the different metrics, Levenshtein and sequence match matched best with 8 out of 30 matches, although the score is still low. Manhattan distance and Edit Distance had the most number of entries in the top 10, with Manhattan distance sum having 5 entries while the mean version having 3. Edit Distance has a total of 3 for the full length and 3 for the transitions. LCS had the worst performance with all its entries below the top 10 and sequence match performed decent with half of its entries above the top 10 and the rest below.

There resulted a total of 12 entries for the non-transitions and 8 for transitions which means that testing only the transitions for comparison is not enough to find similarities as its results are more inconsistent compared to that of the original length.

Table 5.12: Metric Evaluation from Pairwise Symphonies

Metric 1	Metric 2	Matches
Manhattan Distance Mean	Manhattan Distance Sum	10
Manhattan Distance Mean	LCS Truncated	1
Manhattan Distance Mean	Sequence Match	1
Manhattan Distance Sum	LCS Truncated	0

Manhattan Distance Sum	Sequence Match	0
LCS Truncated	Sequence Match	0
Manhattan Distance Transition Sum	Manhattan Distance Mean	2
Manhattan Distance Transition Sum	Manhattan Distance Sum	3
Manhattan Distance Transition Sum	LCS Truncated	0
Manhattan Distance Transition Sum	Sequence Match	1
Edit Distance Full	Manhattan Distance Mean	5
Edit Distance Full	Manhattan Distance Sum	6
Edit Distance Full	LCS Truncated	0
Edit Distance Full	Sequence Match	4
Edit Distance Full	Manhattan Distance Transition Sum	2
Edit Distance Transitions	Manhattan Distance Mean	3
Edit Distance Transitions	Manhattan Distance Sum	3
Edit Distance Transitions	LCS Truncated	0
Edit Distance Transitions	Sequence Match	8
Edit Distance Transitions	Manhattan Distance Transition Sum	2
Edit Distance Transitions	Edit Distance Full	5

In order to evaluate which composers had a wider impact to other symphonies, we tabulate the average distances or percentage per composer per era to see which composer had the least distance or the highest percentage. If different metrics produce similar results, then we can say that those metrics produced good results. Table 5.13 shows the average number of edits per composer, under each era. The table shows that Gabrieli (P1C3) has the lowest average Levenshtein distance from all of the composers across all eras while Rachmaninoff (P5C2) has the largest. It can be seen that composers from the 20th Century era (P5) returned the largest results, this could be due to the fact that the symphonies are longer than the other symphonies, which results to them having a longer trajectory string. In order to address the issue, the researchers have normalized the Levenshtein distances by dividing the results by the length of the longer trajectory string.

Table 5.13: Average Levenshtein Distance per Composer

Row	Baroque	Classical	19th Century	Romantic	20th Century
C1	1191.4	1120.7	1420.6	3097.2	2447.4
C2	724.5	1204	1309.1	2232.6	4005.6
C3	468.3	815.3	1424.7	3308.7	3380.3
C4	1018	1755.8	1639.6	2451	3133.3
C5	503	2378.3	1852.2	1559.4	3863

Table 5.14: My caption

Row	Baroque	Classical	19th Century	Romantic	20th Century
C1	0.854	0.439	0.693	0.705	0.436
C2	0.743	0.681	0.721	0.701	0.66-1
C3	0.857	0.538	0.442	0.7101	0.611
C4	0.781	0.569	0.635	0.755	0.569
C5	0.736	0.63	0.717	0.7	0.649

The researchers experimented on compressing the trajectory string, only taking into consideration the different transitions from letter to letter, ignoring the number of times the letter was repeated. This compressed trajectory string will now be compared using Levenshtein distance. Table 5.15 shows the average Levenshtein distances per composer using the compressed trajectory string. Viadana (P1C5) has the lowest average Levenshtein distance.

Table 5.15: Average Levenshtein Distance (Compressed) per Composer

Row	Baroque	Classical	19th Century	Romantic	20th Century
C1	160.7	422.6	229.5	852.3	702.3
C2	272.1	623	199.1	674.4	1736.7
C3	111.2	191.7	509.7	260.5	1547.7
C4	228.3	795.6	290.1	428.1	1583.2
C5	40.1	1448.3	403.2	302.1	1581.6

The compressed trajectory strings also underwent normalized Levenshtein distance and results are shown in Table 5.16. Antheil (P5C1) is shown to have the smallest average Levenshtein distance. It also can be noted that having a low Levenshtein distance does not not guarantee having a low normalized Levenshtein distance. In this case,

Table 5.16: Average Normalized Levenshtein Distance (Compressed) per Composer

Row	Baroque	Classical	19th Century	Romantic	20th Century
C1	0.873	0.58	0.624	0.593	0.319
C2	0.697	0.641	0.693	0.54	0.621
C3	0.807	0.382	0.579	0.626	0.532
C4	0.64	0.485	0.54	0.722	0.492
C5	0.559	0.565	0.676	0.584	0.544

Similarly, the result from Manhattan distance was tabulated to show the average distances of each composer per era as seen in Table 5.17. The result shows that Gabrieli of Baroque era (P1C3) had the smallest distance value using the Manhattan while Schubert of Romantic era (P4C3) had the largest. This means that Gabrieli had symphonies that are closer to more symphonies than by other composers while Schubert had symphonies that are more dissimilar to other symphonies. Baroque era, in general, also had overall smaller distances compared to other eras while Romantic era had the largest.

Table 5.17: Average Manhattan Distance per Composer

Row	Baroque	Classical	19th Century	Romantic	20th Century
C1	8166.221	15215.32	10140.51	15769.45	23068.61
C2	6089.764	8331.856	13083.8	14746.23	19661.5
C3	4140.392	9954.428	17667.8	27076.32	18392.58
C4	7199.323	16218.67	11979.14	19391.64	20215.49
C5	4918.109	17404.75	12183.51	13561.83	22579.82

Using the normalized Manhattan distance results with the same procedure as above, it can be seen in Table 5.18 that this time, Viadana of Baroque era (P1C5) had the smallest distance, although Gabrieli, the smallest distance from the non-normalized manhattan distance result, still had a very small distance compared to most composers. This time, however, Antheil of 20th Century had the largest distance instead of Schubert

Table 5.18: Average Normalized Manhattan Distance per Composer

Row	Baroque	Classical	19th Century	Romantic	20th Century
C1	491.3077674	2117.378009	1291.064646	3230.844887	6138.347886
C2	905.0273959	2499.334816	1299.300606	3090.077958	4774.202967
C3	461.8045741	2436.608763	2771.299898	2163.809725	4931.113653
C4	1279.07484	3778.909272	1838.724787	2024.689936	5613.785691
C5	410.6783212	4618.480295	1784.439225	1848.743024	5857.821717

Chapter 6

Conclusion

The results of t-SNE produced good visualizations that represented each symphony, composer, era well. The result of using t-SNE provided a good substitute for SOM as its results had the same characteristics while also being fast and almost the same overall visual maps. The colored maps, however, did not improve upon the previous visualization that SOMphony has provided, since the points still overlap each other as time progresses. Aside from this, using visual results is not enough to compare two different symphonies, there is still the need to support the visual observations by quantitative metrics.

Among the metrics tested for comparison of symphonies in Table 5.12 , two metrics had the most overall matches with other metrics as shown in Chapter 5. Both the Manhattan distance and Levenshtein (Edit-Distance) had the most top matches; therefore, we can conclude that among the metrics tested, both these metrics produced the best results. Longest Common Subsequence performed the worst no matter what methodology was used, truncated, full-length, or transitions. Sequence match performed average as its entries are split above and below the top ten.

Prior to the research, it was hypothesized that using simply the transitions instead of all the points might also produce good comparisons; however, as shown in Chapter 5s Table 5.12, majority of the entries above the top ten are the non-transition tests. We cannot say however that comparing with transitions is generally bad, some transition tests in the metrics also produced good results even if they are in the minority.

Even though this researchs results point to these conclusions, it does not mean that the metrics that were deemed bad are always bad when comparing music in

general quantitatively. Some factors pour in such as the research methodology followed in this research may have affected the result either positively or poorly. For future works, it is highly encouraged to either alter the research methodology or test plenty more metrics to further test music comparisons.

Appendix A

Research Ethics Documents

This section contains all documents related to research ethics.

DE LA SALLE UNIVERSITY
General Research Ethics Checklist

This checklist is to ensure that the research conducted by the faculty members and students of De La Salle University is carried out according to the guiding principles outlined in the Code of Research Ethics of the University. The investigator is advised to refer to the De La Salle University Code of Research Ethics and Guide to Responsible Conduct of Research before completing this checklist. Statements pertinent to ethical issues in research should be addressed below. The checklist will help the researchers and evaluators determine whether procedures should be undertaken during the course of the research to maintain ethical standards. The University's Guide to the Responsible Conduct of Research provides details on these appropriate procedures.

Details of the Research	
Students	Cruz, Edwardo Dionisio, Jefferson Fukouka, Kenji Portales, Naomi
Thesis Adviser	Flores, Fritz
Department	Software Technology Department
Title of the Research	Music Visualization Using Projections to 2D Maps
Term(s) and Academic year in which research is to be conducted	AY 2017-2018 Term 1,2,3

This checklist must be completed AFTER the* De La Salle University Code of Ethics *has been read and BEFORE gathering data.

Questions	**Yes**	**No**
1. Does your research involve human participants (this includes new data gathered or using pre-existing data)? If your answer is **yes**, please answer **Checklist A (Human Participants).**		✔
2. Does your research involve animals (non-human subjects)? If your answer is **yes**, please answer **Checklist B (Animal Subjects).**		✔
3. Does your research involve Wildlife? If your answer is **yes**, please answer **Checklist C (Wildlife)**.		✔
4. Does your research involve microorganisms that are infectious, disease causing or harmful to health? If your answer is **yes**, please answer **Checklist D (Infectious Agents).**		✔

5. Does your research involve toxic/chemicals/ substances/materials? If your answer is **yes**, please answer **Checklist E (Toxic Agents).**		✔

Research with Ethical Issues to address:

If you have a YES answer to any of the above categories, you will be required to complete a detailed checklist for that particular category. A YES answer does not mean the disapproval of your research proposal. By providing you with a more detailed checklist, we ensure that the ethical concerns are identified so these can be addressed in adherence to the University Code of Ethics.

Declaration of Conflict of Interest

[✔] I do not have a conflict of interest in any form (personal, financial, proprietary, or professional) with the sponsor/grant-giving organization, the study, the co-investigators/personnel, or the site.

[ ] I have a personal/family or professional interest in the results of the study (family members who are co-proponents or personnel in the study, membership in relevant professional associations/organizations).

Please describe the personal/family or professional interest:

[ ] I have propriety interest vested in this proposal (with the intent to apply for a patent, trademark, copyright, or license)

Please describe propriety interest:

[ ] I have significant financial interest vested in this proposal (remuneration that exceeds P250,000.00 each year or equity interest in the form of stock, stock options or other ownership interests).

Please describe financial interest:

Declaration

We certify that we have read and understand the De La Salle University Code for the Responsible Conduct of Research and will abide by the ethical principles in this document. We will submit a final report of the proposed study to the DLSU-Research Ethics Office. We will not commence with data collection until we receive an ethics review approval from the College Research Ethics Committee.
Name and Signature of Student 1 Name and Signature of Student 2 Name and Signature of Student 3 Name and Signature of Student 4

Endorsement from thesis adviser to the thesis panel for proposal defense…
Name and Signature of Adviser Date

Endorsement from thesis adviser to the thesis panel for final defense… This is to certify that the research was conducted in a manner that adheres to ethical research standards. I am thus endorsing the group for final defense.
Name and Signature of Adviser Date

RESEARCH ETHICS CLEARANCE FORM For Thesis Proposals[1]	
Names of student researcher/s :	*Cruz, Edwardo* *Dionisio, Jefferson* *Fukuoka, Kenji* *Portales, Naomi*
College:	College of Computer Studies
Department:	Software Technology Department
Course:	BS Computer Science with specialization in Software Technology
Expected duration of project:	from: September 2017 to: July 2018
Ethical considerations *None*	
To the best of our knowledge, the ethical issues listed above have been addressed in the research.	

Name and signature of adviser/mentor
Date:

Name and signature of panelist
Date:

Name and signature of panelist
Date:

[1]The same form can be used for the reports of completed projects. The appropriate heading need only be used.

Appendix B

Turnitin Similarity Report

This section consists of the first page of the Turnitin Originality Report.

Music Visualization Using Projections to 2D Maps

ORIGINALITY REPORT

18%	11%	11%	7%
SIMILARITY INDEX	INTERNET SOURCES	PUBLICATIONS	STUDENT PAPERS

PRIMARY SOURCES

1	www.jmlr.org Internet Source	2%
2	Arnulfo Azcarraga, Arturo Caronongan, Rudy Setiono, Sean Manalili. "Validating the stable clustering of songs in a structured 3D SOM", 2016 International Joint Conference on Neural Networks (IJCNN), 2016 Publication	1%
3	Submitted to De La Salle University - Manila Student Paper	1%
4	"Neural Information Processing", Springer Nature, 2016 Publication	1%
5	Corrêa, Débora C., and Francisco Ap. Rodrigues. "A survey on symbolic data-based music genre classification", Expert Systems with Applications, 2016. Publication	1%
6	netcentric.dlsu.edu.ph Internet Source	1%

Appendix C

List of Features and Definitions

This section consists of the list of features extractable in jAudio and their corresponding definitions.

Spectral Centroid Overall Standard Deviation	The centre of mass of the power spectrum. This is the overall standard deviation over all windows.
Derivative of Spectral Centroid Overall Standard Deviation	Derivative of Spectral Centroid. The centre of mass of the power spectrum. This is the overall standard deviation over all windows.
Running Mean of Spectral Centroid Overall Standard Deviation	Running Mean of Spectral Centroid. The centre of mass of the power spectrum. This is the overall standard deviation over all windows.
Standard Deviation of Spectral Centroid Overall Standard Deviation	Standard Deviation of Spectral Centroid. The centre of mass of the power spectrum. This is the overall standard deviation over all windows.
Derivative of Running Mean of Spectral Centroid Overall Standard Deviation	Derivative of Running Mean of Spectral Centroid. Running Mean of Spectral Centroid. The centre of mass of the power spectrum. This is the overall standard deviation over all windows.
Derivative of Standard Deviation of Spectral Centroid Overall Standard Deviation	Derivative of Standard Deviation of Spectral Centroid. Standard Deviation of Spectral Centroid. The centre of mass of the power spectrum. This is the overall standard deviation over all windows.
Spectral Rolloff Point Overall Standard Deviation	The fraction of bins in the power spectrum at which 85% of the power is at lower frequencies. This is a measure of the right-skewedness of the power spectrum. This is the overall standard deviation over all windows.
Derivative of Spectral Rolloff Point Overall Standard Deviation	Derivative of Spectral Rolloff Point. The fraction of bins in the power spectrum at which 85% of the power is at lower frequencies. This is a measure of the right-skewedness of the power spectrum. This is the overall standard deviation over all windows.
Running Mean of Spectral Rolloff Point Overall Standard Deviation	Running Mean of Spectral Rolloff Point. The fraction of bins in the power spectrum at which 85% of the power is at lower frequencies. This is a measure of the right-skewedness of the power spectrum. This is the overall standard deviation over all windows.
Standard Deviation of Spectral Rolloff Point Overall Standard Deviation	Standard Deviation of Spectral Rolloff Point. The fraction of bins in the power spectrum at which 85% of the power is at lower frequencies. This is a measure of the right-skewedness of the power spectrum. This is the overall standard deviation over all windows.
Derivative of Running Mean of Spectral Rolloff Point Overall Standard Deviation	Derivative of Running Mean of Spectral Rolloff Point. Running Mean of Spectral Rolloff Point. The fraction of bins in the power spectrum at which 85% of the power is at lower frequencies.

	This is a measure of the right-skewedness of the power spectrum. This is the overall standard deviation over all windows.
Derivative of Standard Deviation of Spectral Rolloff Point Overall Standard Deviation	Derivative of Standard Deviation of Spectral Rolloff Point. Standard Deviation of Spectral Rolloff Point. The fraction of bins in the power spectrum at which 85% of the power is at lower frequencies. This is a measure of the right-skewedness of the power spectrum. This is the overall standard deviation over all windows.
Spectral Flux Overall Standard Deviation	A measure of the amount of spectral change in a signal. Found by calculating the change in the magnitude spectrum from frame to frame. This is the overall standard deviation over all windows.
Derivative of Spectral Flux Overall Standard Deviation	Derivative of Spectral Flux. A measure of the amount of spectral change in a signal. Found by calculating the change in the magnitude spectrum from frame to frame. This is the overall standard deviation over all windows.
Running Mean of Spectral Flux Overall Standard Deviation	Running Mean of Spectral Flux. A measure of the amount of spectral change in a signal. Found by calculating the change in the magnitude spectrum from frame to frame. This is the overall standard deviation over all windows.
Standard Deviation of Spectral Flux Overall Standard Deviation	Standard Deviation of Spectral Flux. A measure of the amount of spectral change in a signal. Found by calculating the change in the magnitude spectrum from frame to frame. This is the overall standard deviation over all windows.
Derivative of Running Mean of Spectral Flux Overall Standard Deviation	Derivative of Running Mean of Spectral Flux. Running Mean of Spectral Flux. A measure of the amount of spectral change in a signal. Found by calculating the change in the magnitude spectrum from frame to frame. This is the overall standard deviation over all windows.
Derivative of Standard Deviation of Spectral Flux Overall Standard Deviation	Derivative of Standard Deviation of Spectral Flux. Standard Deviation of Spectral Flux. A measure of the amount of spectral change in a signal. Found by calculating the change in the magnitude spectrum from frame to frame. This is the overall standard deviation over all windows.
Compactness Overall Standard Deviation	A measure of the noisiness of a signal. Found by comparing the components of a window's magnitude spectrum with the magnitude spectrum of its neighbouring windows. This is the overall standard deviation over all windows.

Derivative of Compactness Overall Standard Deviation	Derivative of Compactness. A measure of the noisiness of a signal. Found by comparing the components of a window's magnitude spectrum with the magnitude spectrum of its neighbouring windows. This is the overall standard deviation over all windows.
Running Mean of Compactness Overall Standard Deviation	Running Mean of Compactness. A measure of the noisiness of a signal. Found by comparing the components of a window's magnitude spectrum with the magnitude spectrum of its neighbouring windows. This is the overall standard deviation over all windows.
Standard Deviation of Compactness Overall Standard Deviation	Standard Deviation of Compactness. A measure of the noisiness of a signal. Found by comparing the components of a window's magnitude spectrum with the magnitude spectrum of its neighbouring windows. This is the overall standard deviation over all windows.
Derivative of Running Mean of Compactness Overall Standard Deviation	Derivative of Running Mean of Compactness. Running Mean of Compactness. A measure of the noisiness of a signal. Found by comparing the components of a window's magnitude spectrum with the magnitude spectrum of its neighbouring windows. This is the overall standard deviation over all windows.
Derivative of Standard Deviation of Compactness Overall Standard Deviation	Derivative of Standard Deviation of Compactness. Standard Deviation of Compactness. A measure of the noisiness of a signal. Found by comparing the components of a window's magnitude spectrum with the magnitude spectrum of its neighbouring windows. This is the overall standard deviation over all windows.
Spectral Variability Overall Standard Deviation	The standard deviation of the magnitude spectrum. This is a measure of the variance of a signal's magnitude spectrum. This is the overall standard deviation over all windows.
Derivative of Spectral Variability Overall Standard Deviation	Derivative of Spectral Variability. The standard deviation of the magnitude spectrum. This is a measure of the variance of a signal's magnitude spectrum. This is the overall standard deviation over all windows.
Running Mean of Spectral Variability Overall Standard Deviation	Running Mean of Spectral Variability. The standard deviation of the magnitude spectrum. This is a measure of the variance of a signal's magnitude spectrum. This is the overall standard deviation over all windows.

Standard Deviation of Spectral Variability Overall Standard Deviation	Standard Deviation of Spectral Variability. The standard deviation of the magnitude spectrum. This is a measure of the variance of a signal's magnitude spectrum. This is the overall standard deviation over all windows.
Derivative of Running Mean of Spectral Variability Overall Standard Deviation	Derivative of Running Mean of Spectral Variability. Running Mean of Spectral Variability. The standard deviation of the magnitude spectrum. This is a measure of the variance of a signal's magnitude spectrum. This is the overall standard deviation over all windows.
Derivative of Standard Deviation of Spectral Variability Overall Standard Deviation	Derivative of Standard Deviation of Spectral Variability. Standard Deviation of Spectral Variability. The standard deviation of the magnitude spectrum. This is a measure of the variance of a signal's magnitude spectrum. This is the overall standard deviation over all windows.
Root Mean Square Overall Standard Deviation	A measure of the power of a signal. This is the overall standard deviation over all windows.
Derivative of Root Mean Square Overall Standard Deviation	Derivative of Root Mean Square. A measure of the power of a signal. This is the overall standard deviation over all windows.
Running Mean of Root Mean Square Overall Standard Deviation	Running Mean of Root Mean Square. A measure of the power of a signal. This is the overall standard deviation over all windows.
Standard Deviation of Root Mean Square Overall Standard Deviation	Standard Deviation of Root Mean Square. A measure of the power of a signal. This is the overall standard deviation over all windows.
Derivative of Running Mean of Root Mean Square Overall Standard Deviation	Derivative of Running Mean of Root Mean Square. Running Mean of Root Mean Square. A measure of the power of a signal. This is the overall standard deviation over all windows.
Derivative of Standard Deviation of Root Mean Square Overall Standard Deviation	Derivative of Standard Deviation of Root Mean Square. Standard Deviation of Root Mean Square. A measure of the power of a signal. This is the overall standard deviation over all windows.
Fraction Of Low Energy Windows Overall Standard Deviation	The fraction of the last 100 windows that has an RMS less than the mean RMS in the last 100 windows. This can indicate how much of a signal is quiet relative to the rest of the signal. This is the overall standard deviation over all windows.
Derivative of Fraction Of Low Energy Windows Overall Standard Deviation	Derivative of Fraction Of Low Energy Windows. The fraction of the last 100 windows that has an RMS less than the mean RMS in the last 100 windows. This can indicate how much of a signal is quiet relative to the rest of the signal. This is the overall standard deviation over all windows.

Running Mean of Fraction Of Low Energy Windows Overall Standard Deviation	Running Mean of Fraction Of Low Energy Windows. The fraction of the last 100 windows that has an RMS less than the mean RMS in the last 100 windows. This can indicate how much of a signal is quiet relative to the rest of the signal. This is the overall standard deviation over all windows.
Standard Deviation of Fraction Of Low Energy Windows Overall Standard Deviation	Standard Deviation of Fraction Of Low Energy Windows. The fraction of the last 100 windows that has an RMS less than the mean RMS in the last 100 windows. This can indicate how much of a signal is quiet relative to the rest of the signal. This is the overall standard deviation over all windows.
Derivative of Running Mean of Fraction Of Low Energy Windows Overall Standard Deviation	Derivative of Running Mean of Fraction Of Low Energy Windows. Running Mean of Fraction Of Low Energy Windows. The fraction of the last 100 windows that has an RMS less than the mean RMS in the last 100 windows. This can indicate how much of a signal is quiet relative to the rest of the signal. This is the overall standard deviation over all windows.
Derivative of Standard Deviation of Fraction Of Low Energy Windows Overall Standard Deviation	Derivative of Standard Deviation of Fraction Of Low Energy Windows. Standard Deviation of Fraction Of Low Energy Windows. The fraction of the last 100 windows that has an RMS less than the mean RMS in the last 100 windows. This can indicate how much of a signal is quiet relative to the rest of the signal. This is the overall standard deviation over all windows.
Zero Crossings Overall Standard Deviation	The number of times the waveform changed sign. An indication of frequency as well as noisiness. This is the overall standard deviation over all windows.
Derivative of Zero Crossings Overall Standard Deviation	Derivative of Zero Crossings. The number of times the waveform changed sign. An indication of frequency as well as noisiness. This is the overall standard deviation over all windows.
Running Mean of Zero Crossings Overall Standard Deviation	Running Mean of Zero Crossings. The number of times the waveform changed sign. An indication of frequency as well as noisiness. This is the overall standard deviation over all windows.
Standard Deviation of Zero Crossings Overall Standard Deviation	Standard Deviation of Zero Crossings. The number of times the waveform changed sign. An indication of frequency as well as noisiness. This is the overall standard deviation over all windows.

Derivative of Running Mean of Zero Crossings Overall Standard Deviation	Derivative of Running Mean of Zero Crossings. Running Mean of Zero Crossings. The number of times the waveform changed sign. An indication of frequency as well as noisiness. This is the overall standard deviation over all windows.
Derivative of Standard Deviation of Zero Crossings Overall Standard Deviation	Derivative of Standard Deviation of Zero Crossings. Standard Deviation of Zero Crossings. The number of times the waveform changed sign. An indication of frequency as well as noisiness. This is the overall standard deviation over all windows.
Strongest Beat Overall Standard Deviation	The strongest beat in a signal, in beats per minute, found by finding the strongest bin in the beat histogram. This is the overall standard deviation over all windows.
Derivative of Strongest Beat Overall Standard Deviation	Derivative of Strongest Beat. The strongest beat in a signal, in beats per minute, found by finding the strongest bin in the beat histogram. This is the overall standard deviation over all windows.
Running Mean of Strongest Beat Overall Standard Deviation	Running Mean of Strongest Beat. The strongest beat in a signal, in beats per minute, found by finding the strongest bin in the beat histogram. This is the overall standard deviation over all windows.
Standard Deviation of Strongest Beat Overall Standard Deviation	Standard Deviation of Strongest Beat. The strongest beat in a signal, in beats per minute, found by finding the strongest bin in the beat histogram. This is the overall standard deviation over all windows.
Derivative of Running Mean of Strongest Beat Overall Standard Deviation	Derivative of Running Mean of Strongest Beat. Running Mean of Strongest Beat. The strongest beat in a signal, in beats per minute, found by finding the strongest bin in the beat histogram. This is the overall standard deviation over all windows.
Derivative of Standard Deviation of Strongest Beat Overall Standard Deviation	Derivative of Standard Deviation of Strongest Beat. Standard Deviation of Strongest Beat. The strongest beat in a signal, in beats per minute, found by finding the strongest bin in the beat histogram. This is the overall standard deviation over all windows.
Beat Sum Overall Standard Deviation	The sum of all entries in the beat histogram. This is a good measure of the importance of regular beats in a signal. This is the overall standard deviation over all windows.
Derivative of Beat Sum Overall Standard Deviation	Derivative of Beat Sum. The sum of all entries in the beat histogram. This is a good measure of

	the importance of regular beats in a signal. This is the overall standard deviation over all windows.
Running Mean of Beat Sum Overall Standard Deviation	Running Mean of Beat Sum. The sum of all entries in the beat histogram. This is a good measure of the importance of regular beats in a signal. This is the overall standard deviation over all windows.
Standard Deviation of Beat Sum Overall Standard Deviation	Standard Deviation of Beat Sum. The sum of all entries in the beat histogram. This is a good measure of the importance of regular beats in a signal. This is the overall standard deviation over all windows.
Derivative of Running Mean of Beat Sum Overall Standard Deviation	Derivative of Running Mean of Beat Sum. Running Mean of Beat Sum. The sum of all entries in the beat histogram. This is a good measure of the importance of regular beats in a signal. This is the overall standard deviation over all windows.
Derivative of Standard Deviation of Beat Sum Overall Standard Deviation	Derivative of Standard Deviation of Beat Sum. Standard Deviation of Beat Sum. The sum of all entries in the beat histogram. This is a good measure of the importance of regular beats in a signal. This is the overall standard deviation over all windows.
Strength Of Strongest Beat Overall Standard Deviation	How strong the strongest beat in the beat histogram is compared to other potential beats. This is the overall standard deviation over all windows.
Derivative of Strength Of Strongest Beat Overall Standard Deviation	Derivative of Strength Of Strongest Beat. How strong the strongest beat in the beat histogram is compared to other potential beats. This is the overall standard deviation over all windows.
Running Mean of Strength Of Strongest Beat Overall Standard Deviation	Running Mean of Strength Of Strongest Beat. How strong the strongest beat in the beat histogram is compared to other potential beats. This is the overall standard deviation over all windows.
Standard Deviation of Strength Of Strongest Beat Overall Standard Deviation	Standard Deviation of Strength Of Strongest Beat. How strong the strongest beat in the beat histogram is compared to other potential beats. This is the overall standard deviation over all windows.
Derivative of Running Mean of Strength Of Strongest Beat Overall Standard Deviation	Derivative of Running Mean of Strength Of Strongest Beat. Running Mean of Strength Of Strongest Beat. How strong the strongest beat in the beat histogram is compared to other

	potential beats. This is the overall standard deviation over all windows.
Derivative of Standard Deviation of Strength Of Strongest Beat Overall Standard Deviation	Derivative of Standard Deviation of Strength Of Strongest Beat. Standard Deviation of Strength Of Strongest Beat. How strong the strongest beat in the beat histogram is compared to other potential beats. This is the overall standard deviation over all windows.
Strongest Frequency Via Zero Crossings Overall Standard Deviation	The strongest frequency component of a signal, in Hz, found via the number of zero-crossings. This is the overall standard deviation over all windows.
Derivative of Strongest Frequency Via Zero Crossings Overall Standard Deviation	Derivative of Strongest Frequency Via Zero Crossings. The strongest frequency component of a signal, in Hz, found via the number of zero-crossings. This is the overall standard deviation over all windows.
Running Mean of Strongest Frequency Via Zero Crossings Overall Standard Deviation	Running Mean of Strongest Frequency Via Zero Crossings. The strongest frequency component of a signal, in Hz, found via the number of zero-crossings. This is the overall standard deviation over all windows.
Standard Deviation of Strongest Frequency Via Zero Crossings Overall Standard Deviation	Standard Deviation of Strongest Frequency Via Zero Crossings. The strongest frequency component of a signal, in Hz, found via the number of zero-crossings. This is the overall standard deviation over all windows.
Derivative of Running Mean of Strongest Frequency Via Zero Crossings Overall Standard Deviation	Derivative of Running Mean of Strongest Frequency Via Zero Crossings. Running Mean of Strongest Frequency Via Zero Crossings. The strongest frequency component of a signal, in Hz, found via the number of zero-crossings. This is the overall standard deviation over all windows.
Derivative of Standard Deviation of Strongest Frequency Via Zero Crossings Overall Standard Deviation	Derivative of Standard Deviation of Strongest Frequency Via Zero Crossings. Standard Deviation of Strongest Frequency Via Zero Crossings. The strongest frequency component of a signal, in Hz, found via the number of zero-crossings. This is the overall standard deviation over all windows.
Strongest Frequency Via Spectral Centroid Overall Standard Deviation	The strongest frequency component of a signal, in Hz, found via the spectral centroid. This is the overall standard deviation over all windows.
Derivative of Strongest Frequency Via Spectral Centroid Overall Standard Deviation	Derivative of Strongest Frequency Via Spectral Centroid. The strongest frequency component of a signal, in Hz, found via the spectral centroid. This is the overall standard deviation over all windows.

Running Mean of Strongest Frequency Via Spectral Centroid Overall Standard Deviation	Running Mean of Strongest Frequency Via Spectral Centroid. The strongest frequency component of a signal, in Hz, found via the spectral centroid. This is the overall standard deviation over all windows.
Standard Deviation of Strongest Frequency Via Spectral Centroid Overall Standard Deviation	Standard Deviation of Strongest Frequency Via Spectral Centroid. The strongest frequency component of a signal, in Hz, found via the spectral centroid. This is the overall standard deviation over all windows.
Derivative of Running Mean of Strongest Frequency Via Spectral Centroid Overall Standard Deviation	Derivative of Running Mean of Strongest Frequency Via Spectral Centroid. Running Mean of Strongest Frequency Via Spectral Centroid. The strongest frequency component of a signal, in Hz, found via the spectral centroid. This is the overall standard deviation over all windows.
Derivative of Standard Deviation of Strongest Frequency Via Spectral Centroid Overall Standard Deviation	Derivative of Standard Deviation of Strongest Frequency Via Spectral Centroid. Standard Deviation of Strongest Frequency Via Spectral Centroid. The strongest frequency component of a signal, in Hz, found via the spectral centroid. This is the overall standard deviation over all windows.
Strongest Frequency Via FFT Maximum Overall Standard Deviation	The strongest frequency component of a signal, in Hz, found via finding the FFT bin with the highest power. This is the overall standard deviation over all windows.
Derivative of Strongest Frequency Via FFT Maximum Overall Standard Deviation	Derivative of Strongest Frequency Via FFT Maximum. The strongest frequency component of a signal, in Hz, found via finding the FFT bin with the highest power. This is the overall standard deviation over all windows.
Running Mean of Strongest Frequency Via FFT Maximum Overall Standard Deviation	Running Mean of Strongest Frequency Via FFT Maximum. The strongest frequency component of a signal, in Hz, found via finding the FFT bin with the highest power. This is the overall standard deviation over all windows.
Standard Deviation of Strongest Frequency Via FFT Maximum Overall Standard Deviation	Standard Deviation of Strongest Frequency Via FFT Maximum. The strongest frequency component of a signal, in Hz, found via finding the FFT bin with the highest power. This is the overall standard deviation over all windows.
Derivative of Running Mean of Strongest Frequency Via FFT Maximum Overall Standard Deviation	Derivative of Running Mean of Strongest Frequency Via FFT Maximum. Running Mean of Strongest Frequency Via FFT Maximum. The strongest frequency component of a signal, in Hz, found via finding the FFT bin with the highest

	power. This is the overall standard deviation over all windows.
Derivative of Standard Deviation of Strongest Frequency Via FFT Maximum Overall Standard Deviation	Derivative of Standard Deviation of Strongest Frequency Via FFT Maximum. Standard Deviation of Strongest Frequency Via FFT Maximum. The strongest frequency component of a signal, in Hz, found via finding the FFT bin with the highest power. This is the overall standard deviation over all windows.
MFCC Overall Standard Deviation	MFCC calculations based upon Orange Cow codeThis is the overall standard deviation over all windows.
Derivative of MFCC Overall Standard Deviation	Derivative of MFCC. MFCC calculations based upon Orange Cow codeThis is the overall standard deviation over all windows.
Running Mean of MFCC Overall Standard Deviation	Running Mean of MFCC. MFCC calculations based upon Orange Cow codeThis is the overall standard deviation over all windows.
Standard Deviation of MFCC Overall Standard Deviation	Standard Deviation of MFCC. MFCC calculations based upon Orange Cow codeThis is the overall standard deviation over all windows.
Derivative of Running Mean of MFCC Overall Standard Deviation	Derivative of Running Mean of MFCC. Running Mean of MFCC. MFCC calculations based upon Orange Cow codeThis is the overall standard deviation over all windows.
Derivative of Standard Deviation of MFCC Overall Standard Deviation	Derivative of Standard Deviation of MFCC. Standard Deviation of MFCC. MFCC calculations based upon Orange Cow codeThis is the overall standard deviation over all windows.
LPC Overall Standard Deviation	Linear Prediction Coeffecients calculated using autocorrelation and Levinson-Durbin recursion. This is the overall standard deviation over all windows.
Derivative of LPC Overall Standard Deviation	Derivative of LPC. Linear Prediction Coeffecients calculated using autocorrelation and Levinson-Durbin recursion. This is the overall standard deviation over all windows.
Running Mean of LPC Overall Standard Deviation	Running Mean of LPC. Linear Prediction Coeffecients calculated using autocorrelation and Levinson-Durbin recursion. This is the overall standard deviation over all windows.
Standard Deviation of LPC Overall Standard Deviation	Standard Deviation of LPC. Linear Prediction Coeffecients calculated using autocorrelation and Levinson-Durbin recursion. This is the overall standard deviation over all windows.
Derivative of Running Mean of LPC Overall Standard Deviation	Derivative of Running Mean of LPC. Running Mean of LPC. Linear Prediction Coeffecients

	calculated using autocorrelation and Levinson-Durbin recursion. This is the overall standard deviation over all windows.
Derivative of Standard Deviation of LPC Overall Standard Deviation	Derivative of Standard Deviation of LPC. Standard Deviation of LPC. Linear Prediction Coeffecients calculated using autocorrelation and Levinson-Durbin recursion. This is the overall standard deviation over all windows.
Method of Moments Overall Standard Deviation	Statistical Method of Moments of the Magnitude Spectrum. This is the overall standard deviation over all windows.
Derivative of Method of Moments Overall Standard Deviation	Derivative of Method of Moments. Statistical Method of Moments of the Magnitude Spectrum. This is the overall standard deviation over all windows.
Running Mean of Method of Moments Overall Standard Deviation	Running Mean of Method of Moments. Statistical Method of Moments of the Magnitude Spectrum. This is the overall standard deviation over all windows.
Standard Deviation of Method of Moments Overall Standard Deviation	Standard Deviation of Method of Moments. Statistical Method of Moments of the Magnitude Spectrum. This is the overall standard deviation over all windows.
Derivative of Running Mean of Method of Moments Overall Standard Deviation	Derivative of Running Mean of Method of Moments. Running Mean of Method of Moments. Statistical Method of Moments of the Magnitude Spectrum. This is the overall standard deviation over all windows.
Derivative of Standard Deviation of Method of Moments Overall Standard Deviation	Derivative of Standard Deviation of Method of Moments. Standard Deviation of Method of Moments. Statistical Method of Moments of the Magnitude Spectrum. This is the overall standard deviation over all windows.
Partial Based Spectral Centroid Overall Standard Deviation	Spectral Centroid calculated based on the center of mass of partials instead of center of mass of bins. This is the overall standard deviation over all windows.
Derivative of Partial Based Spectral Centroid Overall Standard Deviation	Derivative of Partial Based Spectral Centroid. Spectral Centroid calculated based on the center of mass of partials instead of center of mass of bins. This is the overall standard deviation over all windows.
Running Mean of Partial Based Spectral Centroid Overall Standard Deviation	Running Mean of Partial Based Spectral Centroid. Spectral Centroid calculated based on the center of mass of partials instead of center of mass of bins. This is the overall standard deviation over all windows.

Standard Deviation of Partial Based Spectral Centroid Overall Standard Deviation	Standard Deviation of Partial Based Spectral Centroid. Spectral Centroid calculated based on the center of mass of partials instead of center of mass of bins. This is the overall standard deviation over all windows.
Derivative of Running Mean of Partial Based Spectral Centroid Overall Standard Deviation	Derivative of Running Mean of Partial Based Spectral Centroid. Running Mean of Partial Based Spectral Centroid. Spectral Centroid calculated based on the center of mass of partials instead of center of mass of bins. This is the overall standard deviation over all windows.
Derivative of Standard Deviation of Partial Based Spectral Centroid Overall Standard Deviation	Derivative of Standard Deviation of Partial Based Spectral Centroid. Standard Deviation of Partial Based Spectral Centroid. Spectral Centroid calculated based on the center of mass of partials instead of center of mass of bins. This is the overall standard deviation over all windows.
Partial Based Spectral Flux Overall Standard Deviation	Cacluate the correlation bettween adjacent frames based peaks instead of spectral bins. Peak tracking is primitive - whe the number of bins changes, the bottom bins are matched sequentially and the extra unmatched bins are ignored. This is the overall standard deviation over all windows.
Derivative of Partial Based Spectral Flux Overall Standard Deviation	Derivative of Partial Based Spectral Flux. Cacluate the correlation bettween adjacent frames based peaks instead of spectral bins. Peak tracking is primitive - whe the number of bins changes, the bottom bins are matched sequentially and the extra unmatched bins are ignored. This is the overall standard deviation over all windows.
Running Mean of Partial Based Spectral Flux Overall Standard Deviation	Running Mean of Partial Based Spectral Flux. Cacluate the correlation bettween adjacent frames based peaks instead of spectral bins. Peak tracking is primitive - whe the number of bins changes, the bottom bins are matched sequentially and the extra unmatched bins are ignored. This is the overall standard deviation over all windows.
Standard Deviation of Partial Based Spectral Flux Overall Standard Deviation	Standard Deviation of Partial Based Spectral Flux. Cacluate the correlation bettween adjacent frames based peaks instead of spectral bins. Peak tracking is primitive - whe the number of bins changes, the bottom bins are matched sequentially and the extra unmatched bins are ignored. This is the overall standard deviation over all windows.

Derivative of Running Mean of Partial Based Spectral Flux Overall Standard Deviation	Derivative of Running Mean of Partial Based Spectral Flux. Running Mean of Partial Based Spectral Flux. Cacluate the correlation bettween adjacent frames based peaks instead of spectral bins. Peak tracking is primitive - whe the number of bins changes, the bottom bins are matched sequentially and the extra unmatched bins are ignored. This is the overall standard deviation over all windows.
Derivative of Standard Deviation of Partial Based Spectral Flux Overall Standard Deviation	Derivative of Standard Deviation of Partial Based Spectral Flux. Standard Deviation of Partial Based Spectral Flux. Cacluate the correlation bettween adjacent frames based peaks instead of spectral bins. Peak tracking is primitive - whe the number of bins changes, the bottom bins are matched sequentially and the extra unmatched bins are ignored. This is the overall standard deviation over all windows.
Peak Based Spectral Smoothness Overall Standard Deviation	Peak Based Spectral Smoothness is calculated from partials, not frequency bins. It is implemented accortding to McAdams 99 McAdams, S. 1999. This is the overall standard deviation over all windows.
Derivative of Peak Based Spectral Smoothness Overall Standard Deviation	Derivative of Peak Based Spectral Smoothness. Peak Based Spectral Smoothness is calculated from partials, not frequency bins. It is implemented accortding to McAdams 99 McAdams, S. 1999. This is the overall standard deviation over all windows.
Running Mean of Peak Based Spectral Smoothness Overall Standard Deviation	Running Mean of Peak Based Spectral Smoothness. Peak Based Spectral Smoothness is calculated from partials, not frequency bins. It is implemented accortding to McAdams 99 McAdams, S. 1999. This is the overall standard deviation over all windows.
Standard Deviation of Peak Based Spectral Smoothness Overall Standard Deviation	Standard Deviation of Peak Based Spectral Smoothness. Peak Based Spectral Smoothness is calculated from partials, not frequency bins. It is implemented accortding to McAdams 99 McAdams, S. 1999. This is the overall standard deviation over all windows.
Derivative of Running Mean of Peak Based Spectral Smoothness Overall Standard Deviation	Derivative of Running Mean of Peak Based Spectral Smoothness. Running Mean of Peak Based Spectral Smoothness. Peak Based Spectral Smoothness is calculated from partials, not frequency bins. It is implemented accortding to

	McAdams 99 McAdams, S. 1999. This is the overall standard deviation over all windows.
Derivative of Standard Deviation of Peak Based Spectral Smoothness Overall Standard Deviation	Derivative of Standard Deviation of Peak Based Spectral Smoothness. Standard Deviation of Peak Based Spectral Smoothness. Peak Based Spectral Smoothness is calculated from partials, not frequency bins. It is implemented accortding to McAdams 99 McAdams, S. 1999. This is the overall standard deviation over all windows.
Relative Difference Function Overall Standard Deviation	log of the derivative of RMS. Used for onset detection. This is the overall standard deviation over all windows.
Derivative of Relative Difference Function Overall Standard Deviation	Derivative of Relative Difference Function. log of the derivative of RMS. Used for onset detection. This is the overall standard deviation over all windows.
Running Mean of Relative Difference Function Overall Standard Deviation	Running Mean of Relative Difference Function. log of the derivative of RMS. Used for onset detection. This is the overall standard deviation over all windows.
Standard Deviation of Relative Difference Function Overall Standard Deviation	Standard Deviation of Relative Difference Function. log of the derivative of RMS. Used for onset detection. This is the overall standard deviation over all windows.
Derivative of Running Mean of Relative Difference Function Overall Standard Deviation	Derivative of Running Mean of Relative Difference Function. Running Mean of Relative Difference Function. log of the derivative of RMS. Used for onset detection. This is the overall standard deviation over all windows.
Derivative of Standard Deviation of Relative Difference Function Overall Standard Deviation	Derivative of Standard Deviation of Relative Difference Function. Standard Deviation of Relative Difference Function. log of the derivative of RMS. Used for onset detection. This is the overall standard deviation over all windows.
Area Method of Moments Overall Standard Deviation	2D statistical method of momentsThis is the overall standard deviation over all windows.
Derivative of Area Method of Moments Overall Standard Deviation	Derivative of Area Method of Moments. 2D statistical method of momentsThis is the overall standard deviation over all windows.
Running Mean of Area Method of Moments Overall Standard Deviation	Running Mean of Area Method of Moments. 2D statistical method of momentsThis is the overall standard deviation over all windows.
Standard Deviation of Area Method of Moments Overall Standard Deviation	Standard Deviation of Area Method of Moments. 2D statistical method of momentsThis is the overall standard deviation over all windows.
Derivative of Running Mean of Area Method of Moments Overall Standard Deviation	Derivative of Running Mean of Area Method of Moments. Running Mean of Area Method of

	Moments. 2D statistical method of momentsThis is the overall standard deviation over all windows.
Derivative of Standard Deviation of Area Method of Moments Overall Standard Deviation	Derivative of Standard Deviation of Area Method of Moments. Standard Deviation of Area Method of Moments. 2D statistical method of momentsThis is the overall standard deviation over all windows.
Area Method of Moments of MFCCs Overall Standard Deviation	2D statistical method of moments of MFCCsThis is the overall standard deviation over all windows.
Derivative of Area Method of Moments Overall Standard Deviation	Derivative of Area Method of Moments. 2D statistical method of momentsThis is the overall standard deviation over all windows.
Derivative of Running Mean of Area Method of Moments Overall Standard Deviation	Derivative of Running Mean of Area Method of Moments. Running Mean of Area Method of Moments. 2D statistical method of momentsThis is the overall standard deviation over all windows.
Derivative of Standard Deviation of Area Method of Moments Overall Standard Deviation	Derivative of Standard Deviation of Area Method of Moments. Standard Deviation of Area Method of Moments. 2D statistical method of momentsThis is the overall standard deviation over all windows.
Derivative of Area Method of Moments Overall Standard Deviation	Derivative of Area Method of Moments. 2D statistical method of momentsThis is the overall standard deviation over all windows.
Derivative of Running Mean of Area Method of Moments Overall Standard Deviation	Derivative of Running Mean of Area Method of Moments. Running Mean of Area Method of Moments. 2D statistical method of momentsThis is the overall standard deviation over all windows.
Derivative of Standard Deviation of Area Method of Moments Overall Standard Deviation	Derivative of Standard Deviation of Area Method of Moments. Standard Deviation of Area Method of Moments. 2D statistical method of momentsThis is the overall standard deviation over all windows.
Derivative of Area Method of Moments Overall Standard Deviation	Derivative of Area Method of Moments. 2D statistical method of momentsThis is the overall standard deviation over all windows.
Derivative of Running Mean of Area Method of Moments Overall Standard Deviation	Derivative of Running Mean of Area Method of Moments. Running Mean of Area Method of Moments. 2D statistical method of momentsThis is the overall standard deviation over all windows.
Derivative of Standard Deviation of Area Method of Moments Overall Standard Deviation	Derivative of Standard Deviation of Area Method of Moments. Standard Deviation of Area Method

	of Moments. 2D statistical method of momentsThis is the overall standard deviation over all windows.
Area Method of Moments of Log of ConstantQ transform Overall Standard Deviation	2D statistical method of moments of the log of the ConstantQ transformThis is the overall standard deviation over all windows.
Area Method of Moments of ConstantQ-based MFCCs Overall Standard Deviation	2D statistical method of moments of ConstantQ-based MFCCsThis is the overall standard deviation over all windows.
Spectral Centroid Overall Average	The centre of mass of the power spectrum. This is the overall average over all windows.
Derivative of Spectral Centroid Overall Average	Derivative of Spectral Centroid. The centre of mass of the power spectrum. This is the overall average over all windows.
Running Mean of Spectral Centroid Overall Average	Running Mean of Spectral Centroid. The centre of mass of the power spectrum. This is the overall average over all windows.

Appendix D

Symphony Map from Azcarraga & Flores (2016)'s SOMphony

This section contains an image sample of a symphony map

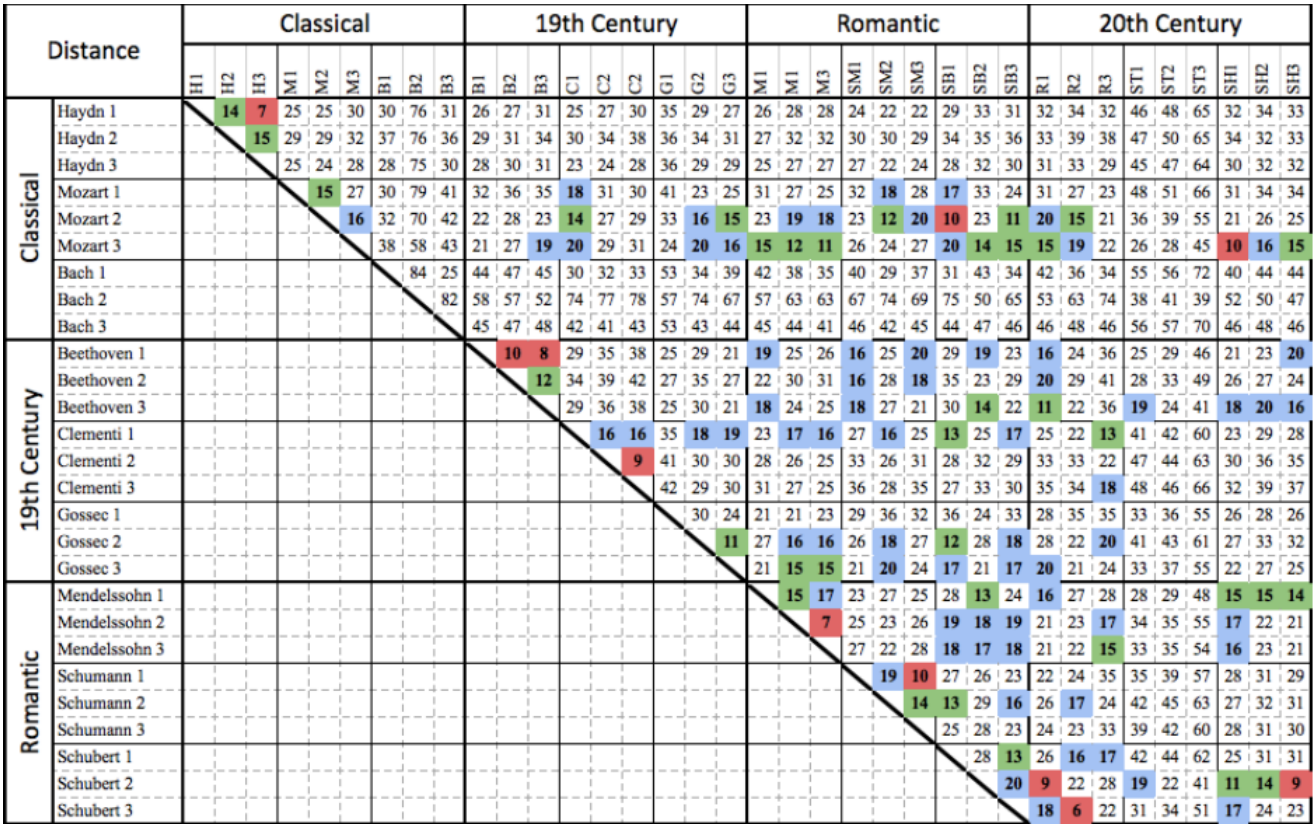

Distance		Classical									19th Century									Romantic									20th Century								
		H1	H2	H3	M1	M2	M3	B1	B2	B3	B1	B2	B3	C1	C2	C2	G1	G2	G3	M1	M1	M3	SM1	SM2	SM3	SB1	SB2	SB3	R1	R2	R3	ST1	ST2	ST3	SH1	SH2	SH3
Classical	Haydn 1		14	7	25	25	30	30	76	31	26	27	31	25	27	30	35	29	27	26	28	28	24	22	22	29	33	31	32	34	32	46	48	65	32	34	33
	Haydn 2			15	29	29	32	37	76	36	29	31	34	30	34	38	36	34	31	27	32	32	30	30	29	34	35	36	33	39	38	47	50	65	34	32	33
	Haydn 3				25	24	28	28	75	30	28	30	31	23	24	28	36	29	29	25	27	27	27	22	24	28	32	30	31	33	29	45	47	64	30	32	32
	Mozart 1					15	27	30	79	41	32	36	35	18	31	30	41	23	25	31	27	25	32	18	28	17	33	24	31	27	23	48	51	66	31	34	34
	Mozart 2						16	32	70	42	22	28	23	14	27	29	33	16	15	23	19	18	23	12	20	10	23	11	20	15	21	36	39	55	21	26	25
	Mozart 3							38	58	43	21	27	19	20	29	31	24	20	16	15	12	11	26	24	27	20	14	15	15	19	22	26	28	45	10	16	15
	Bach 1								84	25	44	47	45	30	32	33	53	34	39	42	38	35	40	29	37	31	43	34	42	36	34	55	56	72	40	44	44
	Bach 2									82	58	57	52	74	77	78	57	74	67	57	63	63	67	74	69	75	50	65	53	63	74	38	41	39	52	50	47
	Bach 3										45	47	48	42	41	43	53	43	44	45	44	41	46	42	45	44	47	46	46	48	46	56	57	70	46	48	46
19th Century	Beethoven 1										10	8	29	35	38	25	29	21	19	25	26	16	25	20	29	19	23	16	24	36	25	29	46	21	23	20
	Beethoven 2											12	34	39	42	27	35	27	22	30	31	16	28	18	35	23	29	20	29	41	28	33	49	26	27	24
	Beethoven 3												29	36	38	25	30	21	18	24	25	18	27	21	30	14	22	11	22	36	19	24	41	18	20	16
	Clementi 1													16	16	35	18	19	23	17	16	27	16	25	13	25	17	25	22	13	41	42	60	23	29	28
	Clementi 2														9	41	30	30	28	26	25	33	26	31	28	32	29	33	33	22	47	44	63	30	36	35
	Clementi 3															42	29	30	31	27	25	36	28	35	27	33	30	35	34	18	48	46	66	32	39	37
	Gossec 1																30	24	21	21	23	29	36	32	36	24	33	28	35	35	33	36	55	26	28	26
	Gossec 2																	11	27	16	16	26	18	27	12	28	18	28	22	20	41	43	61	27	33	32
	Gossec 3																		21	15	15	21	20	24	17	21	17	20	21	24	33	37	55	22	27	25
Romantic	Mendelssohn 1																			15	17	23	27	25	28	13	24	16	27	28	28	29	48	15	15	14
	Mendelssohn 2																				7	25	23	26	19	18	19	21	23	17	34	35	55	17	22	21
	Mendelssohn 3																					27	22	28	18	17	18	21	22	15	33	35	54	16	23	21
	Schumann 1																						19	10	27	26	23	22	24	35	35	39	57	28	31	29
	Schumann 2																							14	13	29	16	26	17	24	42	45	63	27	32	31
	Schumann 3																								25	28	23	24	23	33	39	42	60	28	31	30
	Schubert 1																									28	13	26	16	17	42	44	62	25	31	31
	Schubert 2																										20	9	22	28	19	22	41	11	14	9
	Schubert 3																											18	6	22	31	34	51	17	24	23

Appendix E

t-SNE vs Other Visualizations on MNIST

This section contains image samples of t-SNE Visualization vs Other Techniques on the MNIST Data Set from Maaten & Hinton (2008)'s Visualizing Data Using t-SNE

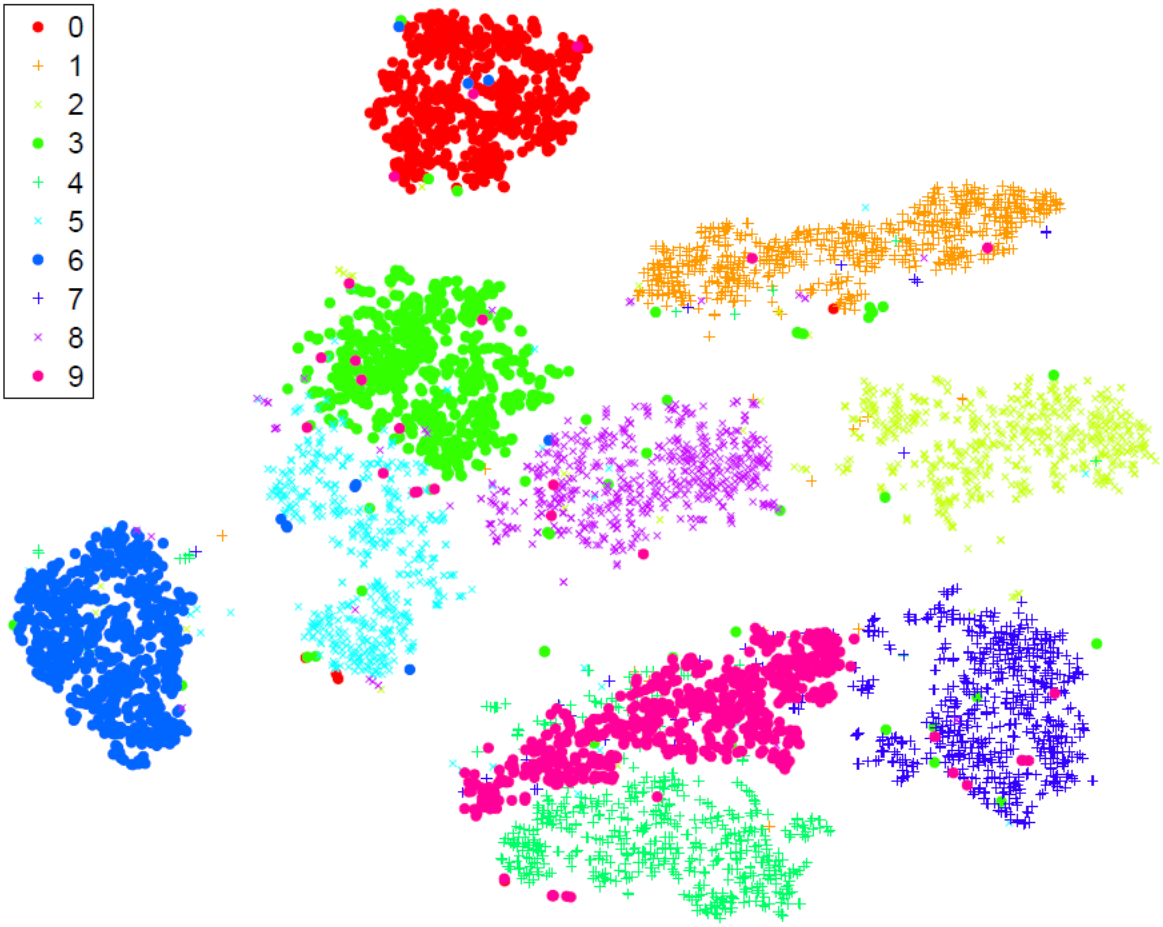

(a) Visualization by t-SNE.

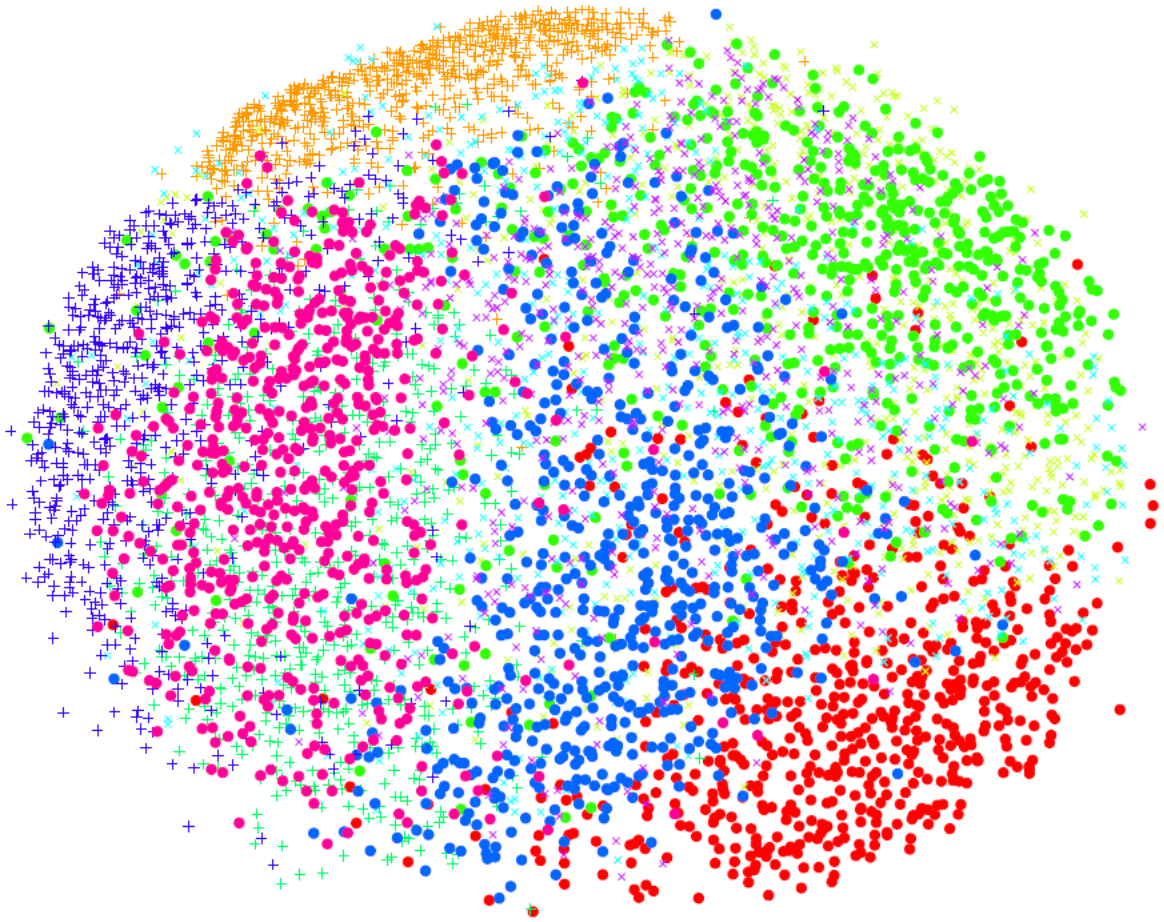

(b) Visualization by Sammon mapping.

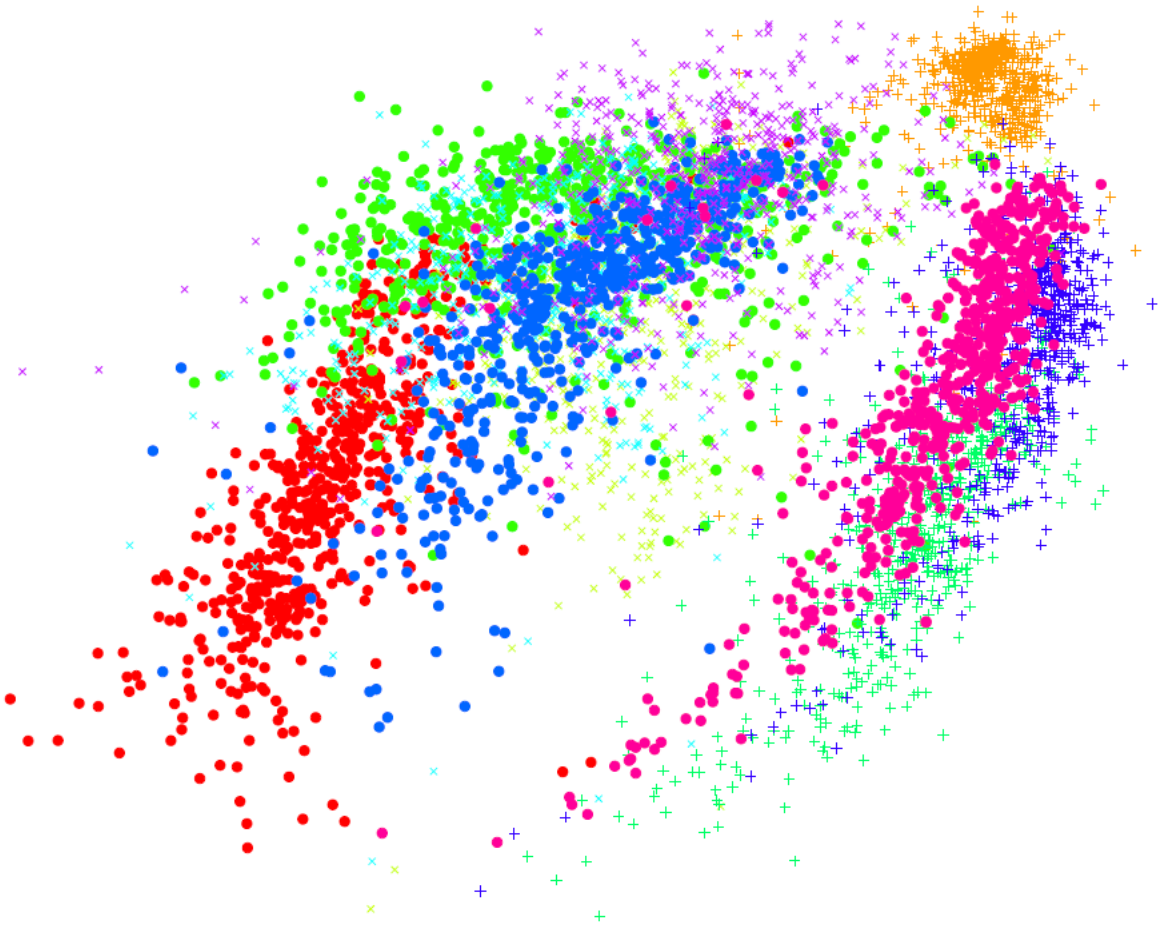

(a) Visualization by Isomap.

Appendix F

Resource persons

Mr. Fritz Kevin S. Flores

Adviser

Computer Technology Department

College of Computer Studies

De La Salle University Manila

fritz.flores@dlsu.edu.ph

Dr. Arnulfo P. Azcarraga

Panelist

Computer Technology Department

College of Computer Studies

De La Salle University Manila

arnie.azcarraga@delasalle.ph

Dr. Judith J. Azcarraga

Panelist

Computer Technology Department

College of Computer Studies

De La Salle University Manila

judith.azcarraga@dlsu.edu.ph

Appendix G

Personal Vitae

Mr. Jefferson Dionisio

+639322215642

jefferson_dionisio@dlsu.edu.ph

Ms. Naomi Portales

+639266796391

naomi_portales@dlsu.edu.ph

Mr. Kenji Fukuoka

+639291722475

kenji_fukuoka@dlsu.edu.ph

Mr. Edwardo Cruz

+639260092665

edwardo_cruz@dlsu.edu.ph